IARIA

HEALTHINFO 2022

The Seventh International Conference on Informatics and Assistive Technologies for Health-Care, Medical Support and Wellbeing

ISBN: 978-1-68558-004-9

October 16 - 20, 2022

Lisbon, Portugal

HEALTHINFO 2022 Editors

Sara Kuppin Chokshi, HITLAB, USA

HEALTHINFO 2022

Forward

The Seventh International Conference on Informatics and Assistive Technologies for Healthcare, Medical Support and Wellbeing (HEALTHINFO 2022), held between October 16th and October 20th, 2022, continued a series of events on particular aspects belonging to health informatics systems, health information, health informatics data, health informatics technologies, clinical practice and training, and wellbeing informatics in terms of existing and needed solutions.

The progress in society and technology regarding the application of systems approaches information and data processing principles, modeling and information technology, computation and communications solutions led to a substantial improvement of challenges in assistive healthcare, public health, and the everyday wellbeing. While achievements are tangible, open issues related to global acceptance, costs models, personalized services, record privacy, and real-time medical actions for citizens' wellbeing are still under scrutiny.

We take here the opportunity to warmly thank all the members of the HEALTHINFO 2022 technical program committee, as well as all the reviewers. The creation of such a high-quality conference program would not have been possible without their involvement. We also kindly thank all the authors who dedicated much of their time and effort to contribute to HEALTHINFO 2022. We truly believe that, thanks to all these efforts, the final conference program consisted of top-quality contributions. We also thank the members of the HEALTHINFO 2022 organizing committee for their help in handling the logistics of this event.

We hope that HEALTHINFO 2022 was a successful international forum for the exchange of ideas and results between academia and industry and for the promotion of progress in the field of informatics and assistive technologies for healthcare, medical support and wellbeing.

HEALTHINFO 2022 Chairs

HEALTHINFO 2022 Steering Committee

Shada Alsalamah, King Saud University, Saudi Arabia
Nelson P. Rocha, University of Aveiro, Portugal

HEALTHINFO 2022 Publicity Chairs

Sandra Viciano Tudela, Universitat Politecnica de Valencia, Spain
Jose Luis García, Universitat Politecnica de Valencia, Spain

HEALTHINFO 2022
Committee

HEALTHINFO 2022 Steering Committee

Shada Alsalamah, King Saud University, Saudi Arabia
Nelson P. Rocha, University of Aveiro, Portugal

HEALTHINFO 2022 Publicity Chairs

Sandra Viciano Tudela, Universitat Politecnica de Valencia, Spain
Jose Luis García, Universitat Politecnica de Valencia, Spain

HEALTHINFO 2022 Technical Program Committee

Djafar Ould Abdeslam, University of Haute Alsace, France
Sherif Abdelwahed, Virginia Commonwealth University, USA
Somayeh Abedian, Ministry of Health and Medical Education, Tehran, Iran
Faris M. Abomelha, King Faisal Specialist Hospital & Research Centre, Kingdom of Saudi Arabia
Miriam Allalouf, Azrieli College of Engineering Jerusalem - JCE, Israel
Jens Allmer, Hochschule Ruhr West, University of Applied Sciences, Germany
João R. Almeida, University of Aveiro, Portugal / University of A Coruña, Spain
Shada Alsalamah, King Saud University, Saudi Arabia
Mustapha Aouache, Telecom Division - Centre de Développement des Technologies Avancées (CDTA), Algiers, Algeria
Khalfalla Awedat, Pacific LutheranUniversity, USA
Mana Azarm, University of Ottawa, Canada
Panagiotis D. Bamidis, Aristotle University of Thessaloniki, Greece
Hugo Barbosa, Lusofona University of Porto / Faculty of Engineering of the University of Porto, Portugal
Fabio Baselice, University of Naples Parthenope, Italy
Arriel Benis, Holon Institute of Technology, Israel
Ahmed Bentajer, National School of Applied Sciences | Abdelmalek Essaad University, Tetouan, Morocco
Vilmos Bilicki, University of Szeged, Hungary
Amine Boufaied, ISITCom | University of Sousse, Tunisia
Guillaume Bouleux, University of Saint Etienne | INSA-Lyon, France
Klaus Brinker, Hamm-Lippstadt University of Applied Sciences, Germany
Tolga Çakmak, Hacettepe University, Turkey
Manuel Campos Martínez, University of Murcia, Spain
Armand Castillejo, STMicroelectronics, France
Rui Pedro Charters Lopes Rijo, Polytechnic of Leiria | INESCC | CINTESIS, Portugal
K.A.D. Chathurangika P. Kahandawaarachchi,Sri Lanka Institute of Information Technology, Sri Lanka
Ayan Chatterjee, University of Agder, Grimstad, Norway
Bhargava Chinni, University of Rochester, USA
Giulia Cisotto, University of Padova, Italy / National Centre for Neurology and Psychiatry of Tokyo, Japan
Alberto Cliquet Jr., UNICAMP / USP, Brazil
Zhou Congcong, Zhejiang University, China
Andrea Corradini, KEA Copenhagen, Denmark

Subhashis Das, Dublin City University, Ireland
Giuseppe De Pietro, Institute for High Performance Computing and Networking (ICAR) - Italian National Research Council (CNR), Italy / Temple University’s College of Science and Technology, Philadelphia, USA
Steven A. Demurjian, The University of Connecticut, USA
Anatoli Djanatliev, University of Erlangen-Nuremberg, Germany
Alexandre Douplik, Ryerson University /St. Michael Hospital, Canada
António Dourado, University of Coimbra, Portugal
Stephan Dreiseitl, University of Applied Sciences Upper Austria, Austria
Hossein Ebrahimpour, University of Kashan, Iran
Mounîm A. El Yacoubi, Telecom SudParis / Institut Polytechnique de Paris, France
Mahmoud Elbattah, University of the West of England Bristol, UK / Université de Picardie Jules Verne, France
Şahika Eroğlu, Hacettepe University, Ankara, Turkey
Gokce Banu Laleci Erturkmen, SRDC A.S., Turkey
Shayan Fazeli, UCLA, USA
(David) Dagan Feng, University of Sydney, Australia
Duarte Folgado, Associação Fraunhofer Portugal Research | NOVA School of Science and Technology - LIBPhys-UNL, Portugal
Sebastian Fudickar, Universität Oldenburg, Germany
Rosalba Giugno, University of Verona, Italy
Alexandra González Aguña, University of Alcala, Spain
María Adela Grando, ArizonaState University, USA
David Greenhalgh, University of Strathclyde, UK
Abir Hadriche, ENIS - Sfax University, Tunisia
Muhammad Hasan, Texas A&m International University (TAMIU), USA
Sara Herrero Jaén, University of Alcalá, Spain
Harry Hochheiser, University of Pittsburgh, USA
Mohamed Hosni, ENSAM | Moulay Ismail University, Meknes, Morocco
Wen-Chen Hu, University of North Dakota, USA
Ming Huang, Mayo Clinic, USA
Fábio Iaione, Universidade Federal de Mato Grosso do Sul, Brazil
Tunazzina Islam, Purdue University, USA
Nawel Jmail, Sfax University, Tunisia
Sheila John, Sankara Nethralaya, India
Ashad Kabir, Charles Sturt University, Australia
Mohamad Kassab, The Pennsylvania State University, USA
Dimitrios G. Katehakis, FORTH Institute of Computer Science, Greece
Eizen Kimura, Medical School of Ehime University, Japan
Boris A. Kobrinskii, Federal Research Center “Computer Science and Control” of the Russian Academy of Sciences, Russia
Sara Kuppin Chokshi, HITLAB (Healthcare Information Technology Lab), USA
Tomohiro Kuroda, Kyoto University Hospital, Japan
Yngve Lamo, Western Norway University of Applied Science, Norway
José Lima, CeDRI & INESC TEC, Portugal
Tatjana Loncar-Turukalo, University of Novi Sad, Serbia
Guillermo H. Lopez-Campos, Wellcome-Wolfson Institute for Experimental Medicine | Queen's University Belfast, UK
Ivan Luiz Marques Ricarte, University of Campinas, Brazil

Wendy MacCaull, St. Francis Xavier University, Antigonish, Canada
Carlos Maciel, University of São Paulo, Brazil
Fabrizio Marangio, ICAR - CNR, Italy
Ana Maria Mendonça, University of Porto / INESC TEC, Portugal
Ciro Martins, University of Aveiro, Portugal
Samuel Botter Martins, Federal Institute of São Paulo, Brazil
Miguel-Angel Mayer, Hospital del Mar Medical Research Institute (IMIM), Barcelona, Spain
Oleg Yu. Mayorov, Ukrainian Association for Computer Medicine | Kharkiv State Medical Academy of Postgraduate Education | Institute of Children and Adolescents Health Protection - Nat. Acad. Med. Sci., Ukraine
Paolo Melillo, University of Campania Luigi Vanvitelli, Naples, Italy
Daniela Micucci, University of Milano - Bicocca, Italy
Enid Montague, DePaul University, USA
Laura Moss, University of Glasgow, UK
Vandana V. Mukherjee, IBM Research - Almaden Research Center, USA
Josephine Nabukenya, Makerere University,Uganda
Nuria Ortigosa, Universitat Politecnica de Valencia, Spain
Nelson Pacheco Rocha, University of Aveiro, Portugal
Danilo Pani, University of Cagliari, Italy
Fulvio Patara, University of Florence, Italy
Alejandro Pazos Sierra, Universisity of A Coruña, Spain
Akila Pemasiri, Queensland University of Technology, Australia
Francesco Pinciroli, Politecnico di Milano / National Research Council of Italy / IEIIT - Istituto di Elettronica e di Ingegneria dell'Informazione e delle Telecomunicazioni, Italy
Salviano Pinto Soares, University of Trás-os-Montes and Alto Douro, Portugal
Ana Margarida Pisco Almeida, University of Aveiro, Portugal
Elaheh Pourabbas, National Research Council of Italy, Italy
Claudia Quaresma, NOVA School of Science and Technology | NOVA University of Lisbon, Portugal
Marco Ivan Ramirez Sosa Moran, Tecnologico Nacional de Mexico, Mexico
Sylvie Ratté, Ecole de technologie supérieure - Université of Québec, Montreal, Canada
Abolfazl Razi, Northern Arizona University, USA
Ulrich Reimer, Eastern Switzerland University of Applied Sciences, Switzerland
Emanuele Rizzuto, SAPIENZA University of Rome, Italy
Sandra Rua Ventura, Center for Rehabilitation Research |School of Health | Polytechnic of Porto, Portugal
Vangelis Sakkalis, Institute of Computer Science - Foundation for Research and Technology (ICS - FORTH), Greece
Ahmad Salehi, Monash University, Australia
Alessandra Scotto di Freca, University of Cassino and Southern Lazio, Italy
Jayanthi Sivaswamy, International Institute of Information Technology (IIIT), Hyderabad, India
Berglind Smaradottir, University of Agder, Norway
Pedro Sousa, Nursing School of Coimbra / Center for Innovative Care and Health Technology, Portugal
Zoltán Szlávik, myTomorrows, Netherlands
Toshiyo Tamura, Waseda University, Japan
Adel Taweel, Birzeit University, PS/ King's College London, UK
Rafika Thabet, Grenoble-Alpes | INP | CNRS | G-SCOP, France
Ljiljana Trajkovic, Simon Fraser University, Canada
Diana Trojaniello, Center for advanced technology in health and wellbeing | IRCCS Ospedale San

Raffaele, Milano, Italy
Athanasios Tsanas, University of Edinburgh, UK
Manolis Tsiknakis, Hellenic Mediteranean University / Foundation for Research and Technology Hellas (FORTH), Greece
Ioan Tudosa, University of Sannio, Italy
Jonathan Turner, Technological University Dublin, Ireland
Gary Ushaw, Newcastle University, UK
Ali Valehi, University of Southern California, USA
Maria Vasconcelos, Fraunhofer Portugal AICOS, Portugal
Agnes Vathy-Fogarassy, University of Pannonia, Hungary
Enrico Vicario, University of Florence, Italy
João L. Vilaça, 2Ai - School of Technology | IPCA, Barcelos, Portugal
Klemens Waldhör, FOM Hochschulzentrum Nürnberg, Germany
Shin'ichi Warisawa, The University of Tokyo, Japan
Pengcheng Xi, National Research Council of Canada / University of Waterloo, Canada
Zongxing Xie, Stony Brook University, USA
Sule Yildirim-Yayilgan, Norwegian University of Science & Technology, Norway
Malik Yousef, Zefat Academic College | Galilee Digital Health Research Center (GDH), Israel
Bing Zhou, Snap Research, USA
Stelios Zimeras, University of the Aegean, Greece

Copyright Information

Table of Contents

Quantitative and Qualitative Evaluation of a Navigation Application Adapted to Young People with Intellectual Disabilities

Halisdemir Ufuk
Capgemini Engineering R&I department
Illkirch-Graffenstaden, France
e-mail: ufuk.halisdemir@capgemini.com

Besnier Morgane
Capgemini Engineering R&I department
Illkirch-Graffenstaden, France
e-mail: morgane.besnier@capgemini.com

Zegarra Flores Jesus
Capgemini Engineering R&I department
Illkirch-Graffenstaden, France
e-mail: jesus.zegarraflores@capgemini.com

Coutant Rémi
Centre Ressources Enfance & Adolescence
ADAPEI du Territoire de Belfort, Belfort, France
e-mail: r.coutant@adapei90.fr

***Abstract*— The "ADAPEI Transport" app is an urban navigation tool for young people (10 to 20 years old) with intellectual disabilities. These disabilities lead to memory, time, and space perception problems. Using this tool, these young people learn how to use public transport and navigate in the city independently thanks to a reference path created by an educator. Along the path, steps are recorded to help the user interact with his/her environment in the navigation part. Currently, we are in the test and evaluation phase of the project for the navigation part. The aim of this article is to show the evaluation methods we have created (Python tool and questionnaire) to have feedback from real tests and to test the efficiency of the app. In fact, the app collects data from Inertial Measurement Unit (IMU) sensors and Global Positioning System (GPS), allowing to replay the journey done in a real test. The first results using the app in a real situation with a disabled youth and an educator are very encouraging. Additionally, thanks to the questionnaire and the Python tools developed to qualitatively evaluate a journey from user input, we were able to improve the app.**

Keywords - intellectual disability; user interface; mobile app; algorithms.

I. INTRODUCTION

The association ADAPEI Belfort [1], an association of parents, friends and people with intellectual disabilities or affected by mental disorders, and Capgemini Engineering [2] have developed an inclusive application for young adults and people having intellectual disabilities. This collaboration led to the creation of a mobile application which is now used within the association as a tool to help people having intellectual disabilities to take public transport and to navigate independently in urban areas. For these young people, it is often difficult to use standard navigation applications (Google maps, City mapper) because the interface is not adapted, often too complex or with inaccurate information. In addition, they are more likely to lose their phone, which means that they often have low-cost phones, with less accurate sensors and/or poor Internet reception, which can make using these applications even more difficult. The ADAPEI Transport application is in an advanced stage of development and is now in the test and validation part. This app allows people having intellectual disabilities to gain autonomy to walk independently in cities using adapted navigation information and security buttons [3].

The focus of this work is to create methodologies to test the efficiency of the interaction between the interface of the app and people having intellectual disabilities using quantitative and qualitative evaluations. In the state of the art, we have found some articles that evaluate health mobile apps from a qualitative point of view. For example, there is a method called Mobile Apps Rating Scale (MARS) that evaluates the quality of applications according to four components: engagement, functionality, aesthetics, and information quality [4]. However, this method is not necessarily adapted to the evaluation of the app with people having intellectual disabilities for increasing autonomy. Another article explains the use of a tool to analyze the interaction between a navigation app and people with visual impairment [5]. There are different cameras to record the movement and displacement of the person. In our case, adding these cameras could be disturbing and intrusive for the intellectually disabled person.

In this article, we first briefly describe the ADAPEI Transport app. We then present the evaluation method of the application set up for the test and validation phase. In this part, we will present the creation of a questionnaire, the creation of the tool in Python to evaluate the journey in a qualitative way, and the comparison of navigation algorithms to test their efficiencies. Then, we will present the results and, finally, the conclusion.

II. THE ADAPEI TRANSPORT APP

The application is composed of three parts: (i) the creation of a route done by a caregiver and/or young adult with disabilities, (ii) the visualization of this route to learn the steps and (iii) the navigation part. The first two parts have been tested with encouraging results. In this article, we will focus on the evaluation of the navigation part. The navigation part consists of showing a list of steps in a sequential way, depending on the position of the person. A progress bar is also shown to know if the person is close to getting off the bus or to pressing the stop button. We have implemented two types of navigation algorithms to test their efficiencies: navigation by the nearest position of a step and navigation by circles of steps.

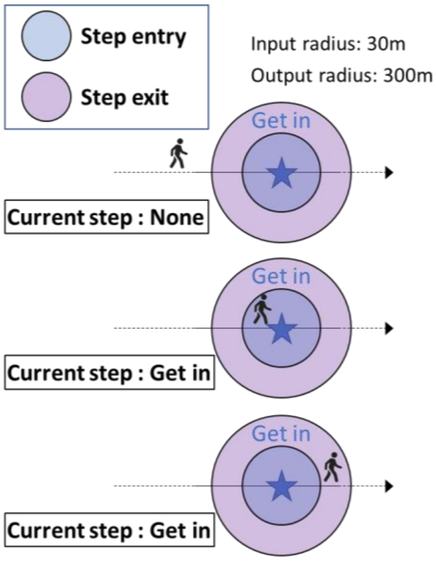

Figure 1. Navigation by circles

During the navigation, a file in JSON format is created containing the navigation data with the coordinates (latitude, longitude, GPS precision and speed) and the values of different sensors (compass, gyroscope, accelerometer). Using this file as input, we developed a tool (coded in Python) to replay the journey, to know when information is launched on the screen and to determine the behavior the user adopts.

III. METHODOLOGY

A. Questionnaire

To make a qualitative evaluation, a questionnaire was created. This questionnaire is filled by a caregiver who will follow the child/young adult during real-life tests. It has three objectives: to note the problems that the user may have during the journey (discomfort, direction problems, hesitations), to note the problems related to the application (bugs, display errors) and to propose improvements.

The questionnaire is inspired by various articles talking about metrics used in the qualitative evaluation of mobile apps [6][7]. We have chosen different metrics, such as 'efficiency, understanding, satisfaction'. The questionnaire is divided into 3 parts:

- Profile of the young person: age, transport habits, level of autonomy.
- Test process: errors in the journey, hesitation, intervention of the companion.
- The application: bugs encountered, remarks, inconsistency of information.

B. Python tool

To perform functional tests of the mobile application, a Java Android emulator in Android Studio was created replaying a trip using a GPS eXchange Format (GPX) file. This file is created when the user launches a trip on their phone. However, the Android emulator does not consider important elements such as speed, GPS accuracy and a set of data from the IMU sensors. This is the main reason why a more sophisticated emulator using Python has been developed. The purpose of this interface is to replay the trips in order to compare the navigation algorithms and to find possible problems/bugs and/or improvements.

The tool allows to recover many files: one to have the initial base of the journey, another to detect the changes of directions and segments to distinguish walking paths from bus paths, and the JSON file to replay the route done by the child using sensors data.

C. Algorithm comparison and slowdown detection

1) Navigation by the nearest position of steps

To know which step is the current step, the algorithm computes the distances between the current position of the person to all the positions of every steps. The step with the smallest distance is the current step and previous steps disappear.

2) Navigation by circles of steps

This algorithm aims to be as close as possible to reality. It has two circles per step which differentiate the entry from the exit of the step. Each circle radius depends on the type of the step. In this version, we detect if we are in the circle or not (see Figure 1). When we exit a step, all the previous steps disappear.

Example: *To enter the step "Get into the bus" you must be less than 30m away from the position of the step and to validate it, you must be inside the bus and more than 300m away from the position of the step and at a speed ~70km/h (bus speed).*

3) Slowing down detection

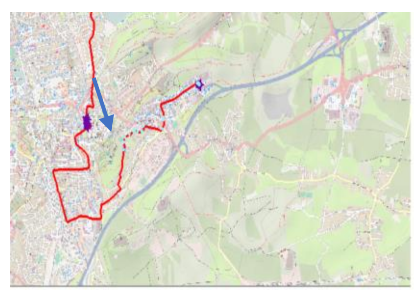

Figure 2. Belfort route, navigation by the nearest position of steps

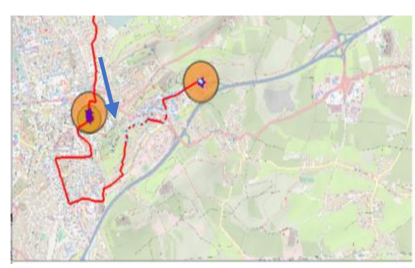

Figure 3. Belfort route, navigation by circles of steps

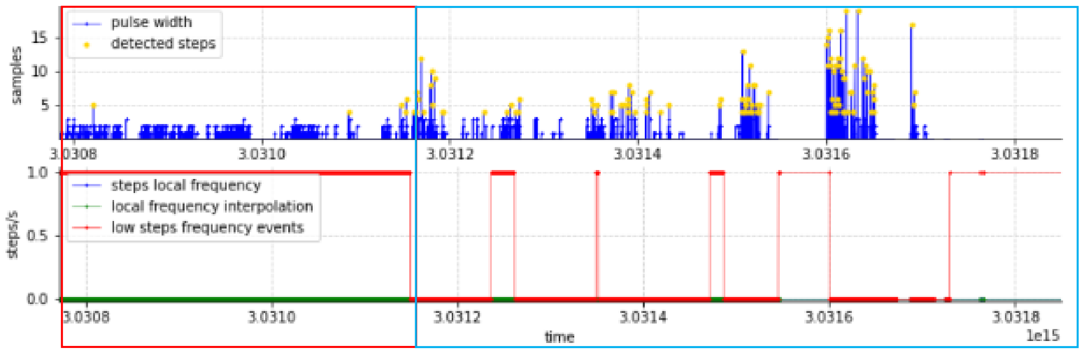

Figure 4. Slowdown detection graph

When a caregiver creates a journey using the app, a file that allows to split the trip into different segments and to differentiate the pedestrian segments from the bus/tramway segment is recorded. Using this file and the accelerometer data, we set up a slowdown detection in order to tell if the user could have some hesitation during the trip. The slowdown is detected using the frequency of the walking. A low step frequency can be considered as an hesitation of the person.

To identify if the user is walking at a low steps frequency, the compound acceleration is calculated thanks to the accelerometers data on three axes (X, Y, Z) (1).

$$a_{comp} = a_x + a_{xy} + a_z \quad (1)$$

The mean steps frequency for each segment is used to know if the user is walking at a low frequency (2). When the local step frequency is lower than 0.5*mean steps frequency, a low frequency event is raised

$$freq_{local}[i] = \frac{1}{time_{step_{i+1}} - time_{step_i}} \quad (2)$$

This algorithm was developed by our team and has an accuracy of 90% for the step counter [8].

IV. Results

A. Algorithm's comparison

In Figures 2 and 3, we see that, for the same position, the remaining steps are not the same. The algorithm by the nearest step takes the step with the smallest distance. At this point, the closest step is n°7. Therefore, steps 5 (to press on the stop button to alert to get off) and 6 (get off from the bus) are already validated, even though they have not been done. This can mislead the user or confuse them, as they do not see what the steps already validated consist of. Following this observation on this route and three other routes, we conclude that the navigation algorithm by circles seems to better reflect reality because steps 5 and 6 appear/disappear at the right moment when the person is close to getting off.

B. Test in real conditions carried out in Belfort

The objective of this part is to see the errors in real tests using the Python tool and the questionnaire as well as the slowing down of the user which we assume to be user hesitation.

A trajectory was created in Belfort (see Figure 2) with some characteristics: 13 km; a bus change, two moments to press on the stop button. Before being able to do the tests in real conditions, there is a whole learning process that the specialist does with the young person. Currently, we have only had one test feedback giving interesting results. The test was carried out with a teenager having intellectual disabilities who is not used to take public transport, but with a good level of mobility. He seemed comfortable during the test, but had a problem which forced the educator to act. The problem came from a confusion if it was the moment to press on the stop button or not. The progress bar was not completely full when the stop button should have been pressed. This problem led to changes in the application. Overall, this test was a success because, apart from this problem, everything else went well. In the questionnaire, it was also suggested to make a modification to have a bigger size of the step image to have a clear understanding of the current step to follow.

Thanks to the interface, we were able to visualize the problem with the progress bar that was wrongly implemented in the application while it was working in the Python tool. The tool made it easier to understand the error.

Figure 4 shows the slowdown. The segment in red represents the second bus trip and the blue corresponds to the last pedestrian part. We can see that the person does not walk on segment 3 as he is in the bus, so we do not have any step detected. On the other hand, we see slowdowns on segment 4 of variable duration. However, these slowdowns are interpreted as hesitations because the questionnaire does not tell anything about them. This can be due to a wait at a red light, for example.

V. Conclusion

In this paper, we developed methodologies to qualitatively and quantitatively test the efficiency of a navigation application designed for people with disabilities. For the qualitative evaluation, we developed a questionnaire is filled by a caregiver who follows the child/young adult during real-life tests. This allows us to get feedback as close as possible from the user's perspective and modify the app when necessary. For the quantitative evaluation, we developed

Python tools that allow to virtually replay a journey with different navigation algorithms to test their efficiency.

The methodology proposed seems to be correct. Thanks to the Python tool, we were able not only to identify problems present in the application, but also to compare the algorithms used for the navigation to see which one was the most efficient thanks to tests carried out on 4 routes.

Even if we only have one feedback on the questionnaire, it gave us very interesting information that allowed us to improve the application. More tests are still necessary to validate our methodology.

In the future, we should improve the slowdown detection using data from the other IMU sensors present on the phone to try to detect real hesitation.

REFERENCES

[1] Capgemini Engineering, France, [online] https://capgemini-engineering.com/fr/fr/, [last access October 2022].

[2] Adapei – Belfort territory, France, [online] https://adapei90.fr/, [last access October 2022].

[3] J. Zegarra Flores et al., “ADAPEI-TRANSPORT: A GPS Based Mobile App for Learning Paths and Improving Autonomy for Young Adults Having Intellectual Disabilities to Take Public Transport”, Computers Helping People with Special Needs. ICCHP 2020. Lecture Notes in Computer, pp. 112-119, 2020.

[4] Y. Terhorst et al., “Validation of the mobile application rating scale (MARS).” PLoS One, 15(11), e0241480, 2020.

[5] I. Maly, J. Balata, O. Krejcir, E. Fuzessery, and Z. Mikovec, “Qualitative measures for evaluation of navigation applications for visually impaired.” In 2015 6th IEEE international conference on cognitive infocommunications (CogInfoCom) , pp. 223-228, 2015.

[6] N. N. Patel and P. Dalal, “Usability evaluation of mobile applications”, International Journal of Engineering Research & Technology (IJERT), 2(11), pp. 299-302, 2013.

[7] R. Alturki and V. Gay, “Usability attributes for mobile applications: a systematic review.” Recent Trends and Advances in Wireless and IoT-Enabled Networks, pp. 53-62, 2019.

[8] J. Z. Flores, S. Cornus, E. Charbonnier, and L. Rasseneur, “Navi Campus: Quantitative Methodology for Evaluating the User Interface of a Navigation App Using Eye Tracker and Smartphone”, in the Proceedings of The Sixth International Conference on Informatics and Assistive Technologies for Health-Care, Medical Support and Wellbeing (HEALTHINFO), IARIA, 2021, pp. 37-40.

 ISBN: 978-1-68558-004-9

COVID-19: Review of Data Analysis

Anthony Dias
Polytechnic Institute of Castelo Branco
6000-767 Castelo Branco, Portugal
e-mail: anthonydias7@gmail.com

Cristiana Barata
Polytechnic Institute of Castelo Branco
6000-767 Castelo Branco, Portugal
e-mail: barata.cris.cb@gmail.com

Filipe Fidalgo
R&D Unit in Digital Services, Applications and Content, Polytechnic Institute of Castelo Branco, Portugal
e-mail: ffidalgo@ipcb.pt

Ângela Oliveira
R&D Unit in Digital Services, Applications and Content, Polytechnic Institute of Castelo Branco, Portugal
e-mail: angelaoliveira@ipcb.pt

Abstract **- The first infection caused by Covid-19 appeared in December 2019 and has infected about 250 million people since. In pandemics, it is essential to model propagation so that it is possible to know how to act to avoid a significant public health problem. Since the appearance of Covid-19, mathematicians, scientists, physicians, and engineers have cooperated in data analysis. This study aims to understand which mathematical models are more relevant and used in this context. Based on Preferred Reporting Items for Systematic Reviews and Meta-Analyses (*PRISMA)* methodology, we will analyse Covid-19 related articles, meeting the results in predicting this pandemic in Portugal and worldwide. All the articles chosen use models or algorithms to perform *prediction*, and we conclude that the Susceptible-Infected-Recovered (SIR) model was the most appropriate and the most used. All the articles have been published up to April 2021.**

Keywords – PRISMA; literature review; Covid-19; prediction; SIR.

I. INTRODUCTION

Humans have been affected by infectious diseases since human behaviours allowed for their spread and, according to [1], there have been reports of episodes of infectious diseases since antiquity. According to [2], an epidemic is the spread of an infectious and contagious disease that develops in a place or region, quickly, causing many victims in a short period of time. A pandemic is an infectious disease that spreads worldwide and attacks at the same time numerous people in many countries.

The Coronavirus that existed before the onset of SARS-CoV also represented a significant public health problem, despite being responsible for only mild respiratory illnesses limited to the upper respiratory tract, such as the common flu. One of the most significant pandemics was the Spanish flu, between 1918 and 1920, in which about 50 million people died. Currently, the world is being affected by the Coronavirus (SARS–CoV–2). Covid-19 is the name attributed by the World Health Organization to the disease caused by the new Coronavirus SARS-COV-2, which can cause severe respiratory infections such as pneumonia. This virus was first identified in humans in late 2019 in the Chinese city of Wuhan. "Being based in more than 100 countries and territories on five continents" [3], it has become one of the biggest challenges of the 21st century. Because the Covid-19 virus has only been present in everyday life since 2019, knowledge about it is still limited. Because it is an acute respiratory infection, SARS-CoV-2 is spread through droplets, respiratory secretions, and direct contact with infected patients. Given this information, all individuals should be considered potential disseminators of the infection, and social distancing and the use of masks should be considered for all as prevention measures. It should be seen that, when there is transmission of the virus, it has an incubation period of 2 to 14 days, verifying the existence of viral excretion about 2 to 3 days before the beginning of symptoms. Even asymptomatic individuals may transmit the virus, although transmission of the infection is unusual. When symptoms are reported, the status of the infected individual must be taken into care, and the most common symptoms may be fever, dry cough, and fatigue. There are also less common symptoms to consider, such as high blood pressure and muscle pain, sore throat, diarrhea, conjunctivitis, headache, loss of taste or smell, skin irritations or discolouration of the fingers or toes. Moreover, in more severe states, patients infected with SARS-CoV-2 may present with difficulty breathing or shortness of breath, chest pressure or pain, speech loss or loss of motor capacity.

For a person to be considered infected, only the symptoms are not enough, and it is necessary to make a positive diagnosis of Covid-19; this is usually done through a molecular test of respiratory secretions. Since the pandemic's beginning, the international scientific community has unified efforts to produce an antiviral treatment that demonstrates positive results; practically every day, numerous methodology articles are published to be developed and potential medicines to combat this virus. At first, due to the lack of a specific and effective treatment against Covid-19, the process was based on symptomatic control and ventilatory support to more acute cases.

More than a year after the SARS-CoV-2 virus was identified, vaccines began to develop in various parts of the world. More than 200 vaccines have been developed, of which 90 have progressed to clinical trials. There are currently four authorised vaccines. Also, in 2020, the vaccination system began, and the entire vaccination process data was housed in the country's existing infrastructure of the Electronic Health Registry. Despite current uncertainty regarding the efficacy and safety of vaccines, studies indicate that they are effective in preventing Covid-19 and in preventing severe disease and death. There is still no certainty about the period of protection they offer or the effectiveness of the various variants.

However, early on, technological tools became great allies for determining preventive measures and for the medical community, as well as for society in general, as these have helped and still help in the detection, prevention, and response against the virus. This pandemic promotes the need for new approaches and technologies. Machine Learning (ML) and Artificial Intelligence (AI) are solutions suitable to the world full of data, contributing to "technological evolution that revolutionises the lives and businesses of all of us" [4]. According to the Organization for Economic Co-operation and Development [5], before the world was even aware of the threat that coronavirus represents, "AI systems had already noticed the outbreak of an unknown type of pneumonia in China", since artificial intelligence is a system that tries to perceive the study environment and takes measures that maximize the chances of success. This tool was used in the management of all stages of the crisis: detection, prevention, response and recovery." These tools have become an indispensable ally in the fight against the pandemic, accelerating the research on treatments, analysing data and other functions like planning, implementing, and evaluating prevention programs.

By analysing articles and work developed by several authors, several epidemiological models have been published to predict its dissemination over the last years of the SARS–CoV–2 pandemic, but there are still uncertainties as to accuracy. The present study will try to understand the characteristics of the most popular models for predicting the evolution of the pandemic. We aim to analyse scientific articles to identify the most used prediction models in a pandemic situation.

This paper is organised as follows. Section 2 presents the details of the methodology of the systematic literature review. Section 3 presents the conclusions and directions for future work.

II. Methodology

This section presents a systematic review of studies that addressed the use of predictions methods for Covid-19 evolution. The review is reported according to the PRISMA statement [6]. It includes the following topics: Research questions (Section A); Inclusion criteria (Section B); Search strategy (Section C); Results (Section D); Data Extraction and Data Analysis (Section E); Discussion (Section F).

A. Research questions

The research questions are as follows: (Q1): What are the existing models/algorithms for the Covid-19 forecast? (Q2): How to make a prediction in an application (web or mobile) for Covid-19? (Q3): What parameters are used for the creation of a Covid-19 forecasting model? (Q4): What advantages do these algorithms bring to the health area and the population?

B. Inclusion criteria

The inclusion criteria of studies and evaluation methods for this review were: (C1): Studies where algorithms applied to data related to Covid-19 are present; (C2): Studies that have calculated formulations applied to data resulting from studies on the theme of Covid-19; (C3): Studies seeking to predict the evolution of the pandemic; (C4): Studies showing assertiveness results of prediction algorithms related to the theme of Covid-19; (C5): Studies that consider the country Portugal; (C6): Studies between 2019 and 2021.

C. Search strategy

Through research and survey of scientific articles in PubMed, ScienceDirect and MedRvix databases, a study was conducted on Covid-19 and the corresponding aspects of this disease. This study made it possible to understand the best practices about data processing, algorithms to be implemented, and the best ways to select the best model. The articles included were published between 2019 - 2021 and selected according to relevance to the proposal of this review. The research terms used to perform this systematic review were: "Covid", "Algorithm", "Forecast", "Portugal", which were chosen and analysed to identify the different types of Covid-19 prediction algorithms that are being used in Portugal. This survey was conducted in April 2021.

D. Results

After the literature search, 136 studies were obtained (after removing five duplicates) and, after applying the inclusion criteria identified in Section 2.2, 49 studies were excluded, resulting in 82 studies. These studies were evaluated in terms of title and abstract, resulting in the exclusion of 28 studies. The full-text evaluation of the remaining 54 studies was performed, excluding 36 studies that did not match the defined inclusion criteria, did not present sufficient information about the algorithm used, or lacked an outcome. The remaining 18 studies are presented in the qualitative and quantitative synthesis.

E. Data Extraction and Data Analysis

Data were extracted from all identified studies using a predefined data format that included: study name, authors, year of publication, date, methods/algorithm, programming language/platforms. Two reviewers extracted the information, and any disagreements were resolved via discussion. Table I shows the extracted data. The characteristics of the included studies are summarized next.

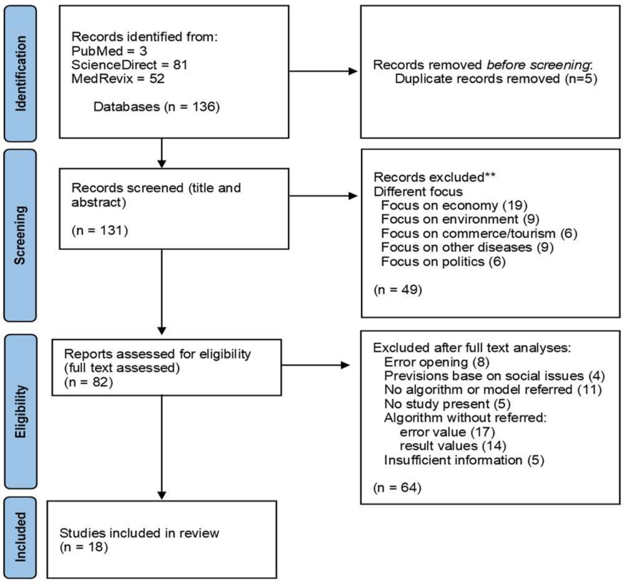

Figure 1. Flow diagram for new systematic reviews (adapted from [6])

TABLE I. EXTRACTED DATA.

Article Name	*Method/ Algorithm*	*Programming Language*
Tracking R of COVID-19: A New Real-Time Estimation Using the Kalman Filter [7]	SIR	R
A Novel Smart City Based Framework on Perspectives for application of Machine Learning in combatting Covid-19 [8]	SIR Random Forest	NA
Extension of a SIR modelling the propagation of Covid-19 in several countries [9]	SIR	R
COVID 19 in Portugal: predictability of hospitalization, ICU and respiratory-assistance needs [10]	Random Forest Decision Tree	Python
Estimation of COVID-19 spread curves integrating global data and borrowing information [11]	SEIR	NA
Data-driven inference of the reproduction number for COVID-19 before and after interventions for 51 European countries [12]	SIR	Python C++
Simplified model of Covid-19 epidemic prognosis under quarantine and estimation of quarantine effectiveness [13]	SIR	R
Covid-19 trajectories Monitoring pandemic in the worldwide context [14]	SIR	R
Estimating the parameters of SIR model of COVID-19 cases in India during lock down periods [15]	SIR	Python
The current COVID-19 wave will likely in the second-line European countries [16]	Random Forest Logistic Regression Bayesian	R
A new fractional mathematical modelling of COVID-19 with the availability of vaccine [17]	SIR SEIR	MATLAB
Data-Driven Mean-Field-Type Game Perspective [18]	SIR SEIR	C++ MATLAB
A computational tool for trend analysis and forecast of the COVID-19 pandemic [19]	Mathematical functions	MATLAB
Forecasting COVID-19 cases based on a parameter-varying stochastic SIR model [20]	SIR	R
When will the Covid-19 pandemic peak? [21]	SIR Linear Regression	R
Sociodemographic predictors of COVID-19 vaccine acceptance: a nationwide US-based survey study [22]	Logistic Regression Artificial Neural Network	NA
Time series forecasting of new cases and new deaths rate for COVID-19 using deep learning methods [23]	Artificial Neural Network	NA
Modelling the impact of SARS-CoV-2 variants and vaccines on the spread of COVID-19 [24]	SIR	MATLAB

The articles in Table I were analyzed, where the prediction methods were identified as well as the programming languages for the development of these methods. This information served as a basis for answering the formulated research questions.

F. Discussion

Over this time, several epidemiological models have been published predicting the spread of the Covid-19 virus, but there are still ambiguities as to accuracy in many cases. One of the most critical aspects of these articles is the development of models designed to help the entire population understand the importance of prevention. Some of the studies contributed to the prediction of the evolution of the pandemic and helped in decision-making. At an early stage of the pandemic, the articles helped to understand how the virus could develop and how important it was for countries to quarantine or not. With all the discoveries made, it is possible to identify trends concerning vaccines and how the pandemic may develop going forward. When analysing the eighteen selected articles, it can be said that the time interval of the studies occurs from 2020 to 2021, as indicated in Figure 2. The most used method was the SIR, consisting of twelve (12) articles; meanwhile, three (3) of the articles chose to use the SEIR, and the same number (3) used the Random Forest method; two (2) articles use logistic regression and Artificial Neural Network, and finally, (1) article used Linear Regression and fminCon, as shown in the graph in Figure 3. The results were obtained with consideration that there may be more than one model in each article. Table II presents the results obtained for models and programming languages used by the authors. Then, with the help of this research, it was possible to realise that many mathematical models can be used to predict epidemiology. These can be Statistical Learning (SL), ML, or Deep Learning (DL). The most significant difference between SL and ML is the purpose. The SL is designed for the different relationships between the variables, while the ML is designed to make predictions as accurate as possible. The DL is an SL method that extracts resources or attributes from raw data. However, information is limited mainly by the fact that Covid-19 is recent. In many of the studies analysed, only pandemic prevention means are indicated, or specific/discrete values, for example, daily cases and not given for a prediction of the evolution of Covid-19, which is the factor that analytical work.

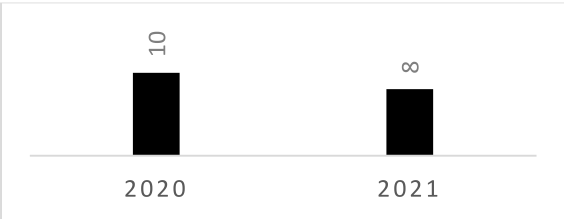

Figure 2. Date of publication of the articles

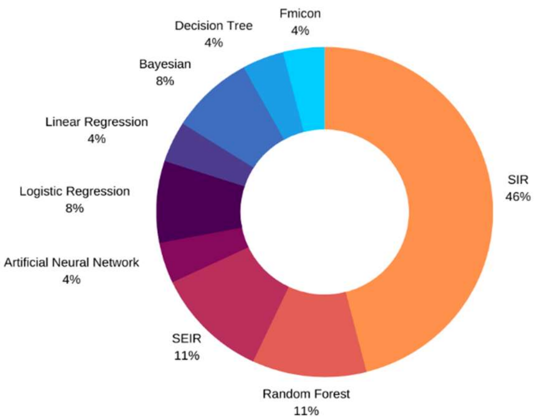

Figure 3. Models/Algorithms

TABLE II. COMPARISON OF ARTICLES RESULTS.

	SIR	Random Forest	Decision Tree	SEIR	Logistic Regression	Bayesian	FmiCon	Linear Regression	Artificial Neural Network
R	**6**	1			1	1		1	1
Phyton	**2**	1	1						
MATLAB	**3**			2			1		1
C++	**2**			1					
Total	**13**	2	1	3	1	1	1	1	2

Based on the information acquired, the answers to the research questions are:

Question 1: What are the existing models/algorithms for the Covid-19 forecast? Practically, every day around the world, new algorithms are used or even generated and may be based on or not existing mathematical models. Regarding the articles that were studied, the SIR model was referenced in the articles [7]-[9][12]-[15][17][18][20][21][24]; in relation to the Random Forest algorithm, it was mentioned in the articles [8][10][16]; the Decision Tree algorithm was exclusively referenced in the article [10]; the variant of the SEIR model appears in the articles [11][17][18]; Logistic Regression is present in the articles [16][22]; Linear Regression was alluded only in the article [21]; the Artificial Neural Network was referenced in the articles [22][23]; finally the Fmincon algorithm in the article [19].

Question 2: How to make a prediction in an application (web or mobile) for Covid-19? A prediction can be made through programs such as MATLAB, which was used to make the predictions in the articles [17]-[19][24]. R was used by the authors of the articles [7][9][13][14][16][20][21]; the articles [10][12][15] use Phyton for prediction, C++ is used in the articles [12][18]. Subsequently, the results obtained are shared and can be implemented in a computerized application content.

Question 3: What parameters are used for the creation of a Covid-19 forecasting model? In a forecast model for Covid-19, the parameters are usually generalised, differentiating between the content with which the treatment is carried out. For their calculations, it is necessary to inform the number of the global population (Susceptible), the number of cases that manifest having the disease (Infected) and the number of the entire population that has managed to overcome so far (Recovered), this information is contained in all eighteen (18) articles analyzed.

Question 4: What advantages do these algorithms bring to the health area and the population? The predictor algorithms emerge in the connection between pure statistics with the computer media of ML. Health benefits from them in collecting more accurate data because this significant advance in data analysis allows a pleasant and symbiotic visualization, contributing to a more effective approach by health professionals [19]. For researchers in this area, these algorithms help them have the means for future analysis of a new eventual pandemic [17] and the population now has access to information.

The articles analyzed stated that the deterministic model most implemented in the case studies was the SIR and will be used for future work. This model [25][26] has different dependencies, which are generally called capital letters such as "S", "I", and "R". In the "SIR" model, "S" represents the group of the population likely to contract the disease, "I" represents the group of the population that contracted the disease and that can transmit it to another individual, infectious group, and the "R" represents the group of the population that recovered from the disease.

 ISBN: 978-1-68558-004-9

The transition rates of individuals between different groups are expressed through derivatives; deterministic models are formulated in terms of systems of differential equations. To make the model more realistic, it is usual to increase the number of compartments to characterize more stages of the disease. For example, in a study on the effect of quarantine on the transmission of infectious disease, the authors introduced to this model the quarantine compartment, "Q", if all infected individuals should pass through the compartment before returning to the compartment of susceptible "S" or recovered "R".

When performing the analysis of articles, several questions arise regarding this model, such as:

• What if the dataset changes regularly?

For this question and looking at the case of Portugal, data is provided by DGS every day, but Rt (Recovered by time) is updated weekly. To combat the fact that data changes regularly, the estimate will be developed weekly, with the preceding; this is the most appropriate solution to understand the data trend. The monthly, or even long-term, estimate for the study object in question is not recommended.

For the prediction of the SIR data-based model, some pros and cons are obtained, which are them:

• Pros: It is a simple model; It is compartment-based; It is based on a dataset during a time window; It is a deterministic model; You do not need many iterations to achieve the desired accuracy.

•Cons: When using the standard SIR model, the "N" corresponds to the total population, being a fixed and global value; Age groups are not distinguished.

It is concluded that a model stands out for the number of times it is mentioned in the articles analysed.

III. Conclusion

Through what was addressed in the previous sections, it is concluded that research is one of the most critical phases of this work because it shows the relevance of mathematical modelling in the study of epidemics, the same starting point for the evolution of this study.

To obtain the results of the realised studies, it should be considered that *Covid-19* is recent and, although there is information about the viruses in this family, there is no information on how the virus will grow. As cited earlier, the pandemic is recent and constantly updated, making it challenging to obtain a detailed response or an approximation of great perceptibility of the predicted results in relation to the actual data. Consequently, the analyst's work is challenging, requiring comparing accurate data with the predicted periods to confirm the forecast's success rate. That is why it is vital that the combinations of virologists' knowledge with ML can help create frameworks to combat Covid-19 and provide better automated solutions to fight against Covid-19. In the processing of data, a segmentation of the research was to be accomplished to carry out a collection of mathematical models that meet the proposed needs, understand the evolution and its factors, and make predictions within the scope of Covid-19. The models used in the articles analysed were systematically organised, considering their characteristics. In general, the analysed models can be accurate and have a minimum error rate. However, they cannot accurately predict what will happen in each situation, as it is theoretically impossible to determine how individuals will adapt their behaviour in the community. Using modelling, it is possible to simulate the propagation, in this case of Covid-19, in each population to estimate the total number of affected individuals.

In the analysed studies, several epidemiological models were published to predict the spread of the pandemic, and there are still uncertainties as to their accuracy. Regarding the mathematical models used, it can be stowed that the authors selected the SIR model, the Random Forest, Decision Tree, Logistic Regression, Linear Regression, Artificial Neural Networks, Fmicon, Bayesian and the SEIR model to carry their studies.

The adoption of preventive measures of public health was essential to reducing the outbreak of this contagious disease. Initially, quarantine was the best preventive measure; studies show that without other resources such as masks or gel alcohol, more than four quarantines were required until a reasonable amount of group immunity was arrived at. With the arrival of vaccines, the picture has changed and, as a result, the number of quarantines has been reduced, and a higher number of immune persons is achieved in a smaller period.

After the research and analysis phase, choosing the most appropriate model to simulate the epidemic outbreak is initiated according to the characteristics of the virus under analysis. The transmission and contagion period are the two characteristics being modelled through their rates, and the values of these characteristics are decisive in the analysis of the outbreak's evolution. These characteristics were best represented by the SIR model, which was the most referred by the authors.

After the analysis of scientific articles and the preference of the method to be implemented, it is concluded that it is essential to understand more about the virus and its history.

For future work, it will be interesting to use the SIR method with the addition of new parameters, such as vaccination.

References

[1] H. R. Thieme, “Mathematics in Population Biology,” Princeton University Press, New Jersey, 2003.

[2] J. Soares, “Etymological and detailed dictionary of biology,” Ed. Scipione, São Paulo, 1993.

[3] World Health Organisation, “Coronavirus disease 2019 (Covid-19): situation report 51,” World Health Organization, Geneve, 2020 [Online]. Available: https://apps.who.int/iris/handle/10665/331475, Mar 2021.

[4] A. V. Joshi, “Machine Learning and Artificial Intelligence,” Springer International Publishing, 2020.

[5] OCDE, "Using artificial intelligence to help combat COVID-19," Organisation for Economic Co-operation and Development, OECD Publishing, Apr. 2020, doi: 10.1787/ae4c5c21-en.
[6] M. Page et al., "The PRISMA 2020 statement: An updated guideline for reporting systematic reviews.," BMJ, vol. 372, Jan. 2021, doi: 10.1136/bmj.n71.
[7] F. Arroyo-Marioli, F. Bullano, S. Kučinskas, C. Rondón-Moreno, "Tracking R of COVID-19: A New Real-Time Estimation using the Kalman filter," Plos One, vol. 16, Jan. 2021, doi: 10.1371/journal.pone.0244474.
[8] H. Chiroma and A. E. Ezugwu, "A Novel Smart City Based Framework on Perspectives for application of Machine Learning in combatting Covid-19," BioMed Res Int, vol. 2021, Sep. 2021, doi: 10.1155/2021/5546790.
[9] M. Lavielle, I. Saclay-Ile-de-France, E. Polytechnique, "Extension of a SIR modelling the propagation of Covid-19 in several countries," medRxiv, vol. 2020, May. 2020, doi: 10.1101/2020.05.17.20104885.
[10] A. Patricio, R. S. Costa, R. Henriques, "COVID 19 in Portugal: predictability of hospitalization, ICU and respiratory-assistance needs," medRxiv, vol. 2020, Sep. 2020, doi: 10.1101/2020.09.29.20203141.
[11] L. Yoon, L. Bowen, B. K. Mallick, "Estimation of COVID-19 spread curves integrating global data and borrowing information," Plos One, vol. 15, Jul. 2020, doi: 10.1371/journal.pone.0244474.
[12] P. Karnakov et al., "Data-driven inference of the reproduction number for COVID-19 before and after interventions for 51 European countries," Swiss Med Weekly, vol. 150, Jul. 2020, doi: 10.4414/smw.2020.20313.
[13] A. Džiugys, M. Bieliunas, G. Skarbalius, E. Misiulis, R. Navakas, "Simplified model of Covid-19 epidemic prognosis under quarantine and estimation of quarantine effectiveness," in Chaos, Solitons & Fractals, vol. 140, Elsevier, p. 162, 2020.
[14] H. Loeffler-Wirth, M. Schmidt, H. Binder, "Covid-19 trajectories – Monitoring pandemic in the worldwide context," Viruses, vol. 12, Jul. 2020, doi: 10.3390/v12070777.
[15] D. K. Bagal, A. Rath, A. Barua, D. Patnaik, "Estimating the parameters of susceptible-infected-recovered model of COVID-19 cases in India during lockdown periods," in Chaos, Solitons & Fractals, vol. 140, Elsevier, pp. 110-154, 2020.
[16] S. Soubeyrand, M. Ribaud, V. Baudrot, D. Allard, D. Pommeret, L. Roques, "The current COVID-19 wave will likely be mitigated in the second-line European countries," medRxiv, vol. 2020, Apr. 2020, doi: 10.1101/2020.04.17.20069179.
[17] P. Kumar, V. Erturk, M. Murillo-Arcila, "A new fractional mathematical modelling of COVID-19 with the availability of vaccine," in Results in Physics, vol. 24, Elsevier, pp. 104-213, 2021.
[18] H. Tembine, "COVID-19: Data-Driven Mean-Field-Type Game Perspective," medRxiv, vol. 2020, Jul. 2020, doi: 10.3390/g11040051
[19] H. Paiva, R. Afonso, F. Caldeira, E. Velasquez, "A computational tool for trend analysis and forecast of the COVID-19 pandemic," Applied Soft Computing, vol. 105, Elsevier, pp. 107-289, 2021.
[19] J. Hespanha, R. Chinchilla, R. Costa, M. Erdal, G. Yang, "Forecasting COVID-19 cases based on a parameter-varying stochastic SIR model," in Annual Reviews in Control, vol. 51, Elsevier, pp. 460-476, 2021.
[20] S. Li and O. Linton, "When will the Covid-19 pandemic peak?," in Journal of Econometrics, vol. 220, Issue 1, Elsevier, pp. 130-157, 2021.
[21] P. Mondal, A. Sinharoy, L. Su, "Sociodemographic predictors of COVID-19 vaccine acceptance: a nationwide US-based survey study," in Public Health, vol. 198, Elsevier, pp. 252-259, 2021.
[22] N. Ayoobi et al., "Time series forecasting of new cases and new deaths rate for COVID-19 using deep learning methods," in Results in Physics, vol. 27, Elsevier, pp. 104-495, 2021.
[23] A. Ramos, M. Vela-Pérez, M. Ferrández, A. Kubik, B. Ivorra, "Modelling the impact of SARS-CoV-2 variants and vaccines on the spread of COVID-19," in Communications in Nonlinear Science and Numerical Simulation, vol. 102, Elsevier, pp. 105-937, 2021.
[24] SNS24 Serviço Nacional de Saúde, "Ministry of Health," 2021. [Online]. Available: https://www.sns24.gov.pt/tema/doencas-infecciosas/covid-19/, Mar 2021.
[25] R. M. Anderson, "Discussion: the Kermack-McKendrick epidemic threshold theorem". Bulletin of mathematical biology, 53(1): 1–32, 1991
[26] H. Tiberiu, L. S. N. Francisco and M.K. Mak, "Exact analytical solutions of the Susceptible-Infected-Recovered (SIR) epidemic model and of the SIR model with equal death and birth rates", Applied Mathematics and Computation, 236:184-194, 2014, https://doi.org/10.1016/j.amc.2014.03.030.

An Ontology-Based Tool for the Analysis of the Social Network for Cancer Outpatients

Rémi Bastide
Champollion University
IRIT - Toulouse
France
Remi.Bastide@irit.fr

***Abstract*— In the framework of a research project funded by INCa (French National Institute for Cancer), a team of sociologists has conducted interviews with cancer outpatients, with the goal of analyzing their social support network and its evolution over time. This paper describes the ontology-driven tool supporting the collection and analysis of this sociological data.**

Keywords: Social support for outpatients; health ontologies.

I. Introduction

The healthcare management of cancer has witnessed dramatical changes in the recent years. With the development of ambulatory treatments and oral chemotherapy, only 10% of anticancer chemotherapy in France is now performed in full hospitalization [1]. There is currently a reduction in hospitalization time, and conventional inpatient treatment is gradually replaced by other less expensive methods, such as home hospitalization or ambulatory care.

Although outpatient medical care favours patient autonomy, it also leads to patients and their relatives carrying a new burden of responsibility in defining and implementing their own care pathways. In the framework of a research project funded by INCa (French National Institute for Cancer), a team of sociologists has conducted interviews with post-cancer outpatients, with the goal of assessing the main hypothesis that the success of a healthcare pathway is increasingly dependent on the "resources" that the patients can mobilize to come to terms with their illness.

These resources are obtained within two major types of networks: those structured around the close relatives and those structured around friendly and professional relationships. The complexity of these networks may vary, and their structure is likely to partly explain the social dynamics observed in disease trajectories. This graph of resources and relationships defines the patient's socio-technical network of support, co-constructed by patients themselves, close acquaintances, health professionals, individual and social environment, and technologies.

In the following sections, we present a tool designed to support the collection and sharing of the information gathered during interviews, and permitting a convenient visualization of the evolution of the patient's social graph over time.

II. Tool Support

In the framework of this project, we have developed a software tool allowing the sociologist investigators to analyze how cancer patients construct their healthcare pathway in connection with the medical care team, but also in continuous interaction with their social supports. At the start of the project, the sociologist partners were transcribing their interviews with patients using a structured Excel® sheet, which was fitted with a detailed usage guide, aimed at enhancing the homogeneity of transcriptions made by different investigators. Although this mode of transcription had several advantages (such as familiarity and flexibility) it proved ill-suited in the long term, mainly due to the use of different terminologies by the investigators, who were using various synonymous terms to transcribe the same resources or relationships, thus hampering the possibility of automatic treatment.

To overcome these problems, and to enable the automatic processing and analysis of the recorded data, we developed a software tool, with the goal of preserving the flexibility of the original process, but also to favor the development and sharing of consistent terminologies between investigators. The tool enables a graphical edition of the patients' social relationship network, which is conceived as a graph of *resources* and *relationships* between resources.

Considering that the consistency of the terminologies used for labeling the resources and relationships are of prime importance for enabling further automatic processing, the conceptual design of the tool is based on ontological approach [2]. In order to reach the objectives of flexibility expressed by the investigators (and confirmed by the analysis of interviews in Excel format), the tool allows for the development of a dynamic ontology of resources and relationships, defined and controlled by the investigators themselves [3], [4].

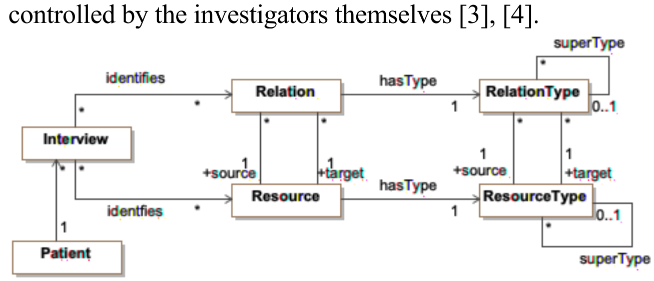

Figure 1. Simplified conceptual model.

A detailed analysis of interviews collected in Excel format led to the conceptual model illustrated in Figure 1, expressed in the Unified Modelling Notation (UML), and was mapped to a relational implementation using the principles described in [5]. For each *patient* under scrutiny, several *interviews* are conducted. During these interviews, the investigators identify the *resources* that are part of the social relationship network of the patient, and the *relationships* between these resources. To ensure the consistency of the interviews' modelling, resources and relationships must be instances of a well-defined ontology, which is illustrated in the right part of Figure 1. This dynamic ontology (*ResourceType* and *RelationType*) constitutes a meta-model for the social network graph of a patient, defining a consistent terminology for resource types (e.g., "informational resource", or "medical act"), and for the legal relationships between resource types (e.g., the relation type "Information acquisition" mandatorily links a resource of type "person" to a resource of type "informational resource". This metamodel can be dynamically extended by the investigators to accommodate new situations, or even be completely redesigned if a new study requires a change of focus regarding the information of interest.

Resource types and relation types are organized as a covariant tree-structure of subtypes [7]. Thus, for instance, the "information acquisition" relationship could relate to a resource of type "Doctor", which is a sub-type of "Person". The software tool allows for a graphical edition of the social relationship graph (Figure 2), and the user interface permits an easy navigation between the successive interviews of a patient, which promotes a visual and intuitive evaluation of the evolution the patient's social graph over time.

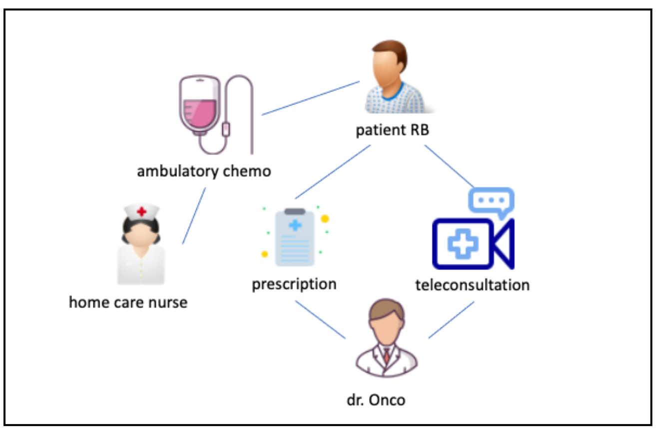

Figure 2. Visual representation of the social graph.

III. Conclusion and Perspectives

The tool has successfully replaced the spreadsheet-based data collection previously used, ensuring the consistency of terminologies amongst sociologist investigators and promoting the sharing of information. The ontology-driven design of the tool opens the possibility of automatic transformation of the collected data in Resource Description Framework (RDF) format [8], which enables the use of specific ontology request languages [9] to integrate network analysis algorithms [10], such as the identification of critical resources.

Acknowledgment

This work is funded by INCa (Institut National du Cancer, France) and is conducted by multi-disciplinary team of researchers in Sociology and in Computer Science.

References

[1] A. Defossez and P. Ducournau, "Patients receiving ambulatory care: a problematic autonomy situation," *Heal. Sociol. Rev.*, pp. 3223–3246, Oct. 2013, doi: 10.5172/HESR.2013.3223.

[2] V. Sugumaran, "Semantic technologies for enhancing knowledge management systems," *Successes Fail. Knowl. Manag.*, pp. 203–213, Jan. 2016, doi: 10.1016/B978-0-12-805187-0.00014-0.

[3] K. Podnieks, "Locally Constrained Ontologies," *Balt. J. Mod. Comput.*, vol. 4, no. 4, Dec. 2016, doi: 10.22364/BJMC.2016.4.4.08.

[4] L. Zhang, S. Xia, Y. Zhou, and Z. Xia, "User denfined ontology change and its optimization," *Chinese Control Decis. Conf. 2008, CCDC 2008*, pp. 3586–3590, 2008, doi: 10.1109/CCDC.2008.4597998.

[5] S. C. Haw, J. W. May, and S. Subramaniam, "Mapping relational databases to ontology representation: A review," *ACM Int. Conf. Proceeding Ser.*, vol. Part F131203, pp. 54–58, Aug. 2017, doi: 10.1145/3134847.3134852.

[6] S. Tang and M. Hanneghan, "A Model-Driven Framework to Support Development of Serious Games for Game-based Learning," in *2010 Developments in E-systems Engineering*, Sep. 2010, pp. 95–100, doi: 10.1109/DeSE.2010.23.

[7] G. Castagna, "Covariance and contravariance: A fresh look at an old issue (a primer in advanced type systems for learning functional programmers)," *Log. Methods Comput. Sci.*, vol. 16, no. 1, Sep. 2020, doi: 10.23638/LMCS-16(1:15)2020.

[8] "Storage and Indexing of RDF Data," *RDF Database Syst.*, pp. 105–144, 2015, doi: 10.1016/B978-0-12-799957-9.00005-5.

[9] "SPARQL 1.1 Query Language." https://www.w3.org/TR/sparql11-query/ (accessed Jun. 01, 2022).

[10] T. Wang *et al.*, "Understanding Graph Sampling Algorithms for Social Network Analysis," in *2011 31st International Conference on Distributed Computing Systems Workshops*, 2011, pp. 123–128, doi: 10.1109/ICDCSW.2011.34.

Monitoring Activities of Daily Living for Maintaining Independent Living in Dementia

Jonathan Turner, Ciarán Nugent, Damon Berry, Dympna O'Sullivan
Department of Computer Science
Technological University Dublin
Dublin, Ireland
Emails: jonathan.turner@tudublin.ie, ciaran.nugent@tudublin.ie, damon.berry@tudublin.ie, dympna.osullivan@tudublin.ie

Michael Wilson, Julie Doyle
NetwellCASALA
Dundalk Institute of Technology
Dundalk, Ireland
Emails: michael.wilson@dkit.ie, julie.doyle@dkit.ie

***Abstract*—Our ability to live independent meaningful lives depends on our ability to perform various activities and to maintain our cognitive functions. Maintaining independent living is important for persons with dementia; it increases self-worth and allows to remain independent and in their own homes for longer. In this article, we describe the activities established as being important for the maintenance of independent living, and methods for monitoring these activities using technology.**

Keywords- dementia; self-monitoring; activities of daily living; independent living.

I. INTRODUCTION

Our work is focused on the development of a tool to extend the period of independent living for Persons Living With Dementia (PLWD) and to enhance Quality of Life (QoL). An integral part of our proposed tool is monitoring of performance of basic activities and cognitive functions. In previous work, we have reviewed tools for monitoring activities for PLWD [1]. In this paper, we describe established measures of activity, together with the reasons for their adoption, with a focus on the importance of maintaining these for PLWDs. We also outine our proposed methods to measure achievement of activities by PLWD in the tool we are developing. Sections II and III give information on means of discovery of measures and how they are used in dementia care. Section IV discusses the use of these measures in our work. We conclude with a discussion in Section V.

II. METHODS

We conducted interviews and focus group with those with expertise in the field (specialist dementia care nurses, occupational therapists from an affiliated University hospital) and conducted a systematic literature review to determine which activities were important in the maintenance of independent living, and which activities were important in maintaining QoL.

III. RESULTS

Activities and functions required for independent living with QoL fell into several clear groups: basic activities necessary for survival; more sophisticated activities requiring a higher level of thought that are necessary for independent living; activities that bring pleasure; and mental abilities that underpin the activities already listed.

A. Activities of Daily Living

Basic survival skills were described by Katz [2] as 'Activities of Daily Living' (ADL). These activities are the most basic activities required to ensure day-to-day survival but are not, in themselves, sufficient to allow for independent living or for a higher quality of life. The activities defined by Katz are shown in Table 1. This table also shows the methods by which we intend to track performance of these activities for PLWD. Where possible, non-invasive sensors are used to track activity; where necessary, PLWD will be asked at intervals about performance of activities via an app.

TABLE I. KATZ'S ACTIVITIES OF DAILY LIVING

Activity name	*Activity description*	*Tracking method*
Bathing	assistance only out of bed independently in bathing a single part or bathes self completely	Humidity sensor in bathroom
Dressing	gets clothes from closets and drawers; puts on clothes, outer garments, braces; manages fasteners; act of tying shoes is excluded	Switch sensor on drawers and/or wardrobe doors
Toileting	gets to toilet; gets on and off toilet; arranges clothes; cleans organs of excretion	Motion sensor in bathroom, flush sensor attached to toilet
Transferring	Moves in and out of bed independently and moves in and out of chair independently	Pressure mat sensor on floor by bed/chair
Continence	urination and defecation entirely self-controlled	App
Feeding	gets food from plate or its equivalent into mouth	App

B. Instrumental Activities of Daily Living

The more sophisticated activities that allow an individual to continue living independently (albeit with some assistance if required) were described by Lawton and Brody [3] as 'Instrumental Activities of Daily Living' (IADL). These are shown in Table 2. Note that the activity description shows the highest level of performance; for example, the Transportation activity allows for 'Travels on public transportation when assisted or accompanied by another' as achieving that IADL. More details on levels of performance for each IADL is given in [5]. We will track these activities by sensor where practical or by asking the PLWD to self-report. Note some IADLs may not be appropriate for some individuals if they have never previously routinely performed an activity (e.g., preparing meals).

TABLE II. INDEPENDENT ACTIVITIES OF DAILY LIVING

Activity name	***Activity description***	***Tracking method***
Telephone	Operates telephone on own- , looks up and dials numbers	Beacon sensor on handset
Shopping	Takes care of all shopping needs independently	App
Food	Plans, prepares and serves adequate meals independently	App
Housekeeping	Maintains house alone or with occasional assistance	App
Transportation	Travels independently -public transportation or drives car	App
Finances	Manages financial matters independently	App
Laundry	Does personal laundry	App

C. Meaningful Activities

The Pleasurable Events Schedule [4] focuses particularly on PLWD; examples include 'being outside' or 'friend visiting'. Note that an ADL or IADL may also be a Meaningful Activity (MA), for example 'Food' (i.e., preparing a meal) may bring a reward of meaning beyond that of the preparing a meal. In our work, we allow PLWD to define their own MAs. For each MA, we determine which IADLs and cognitive functions are required to be exercised.

D. Cognitive Functions

The ability to perform activities that fall in the above groups is underpinned by mental abilities. These have been described in [5] and are shown in Table 3. We do not plan to explicitly track performance of these functions, but instead we determine which IADLs and MAs implicitly exercise these functions and track the performance of these activities to ensure that essential cognitive functions are exercised.

TABLE III. COGNITIVE FUNCTIONS

Table Column Head	
Function name	***Function description***
Perceptual-Motor	Combining sensory input with motor skills
Learning and Memory	Ability to record and retrieve information
Complex Attention	Ability to focus on multiple things
Executive Function	Sequencing, planning and organizing tasks
Language	Communicate and receive communication
Social Cognition	Controlling behavior, recognize social cues

IV. DISCUSSION

There exist long-established sets of ADLs and IADLs. In our proposed tool, we will monitor, and encourage performance of these for PLWDs, and extend an existing set of dementia-specific MAs by allowing PLWDs to suggest their own MAs, to extend their period of independent living for as long as possible with as much QoL as possible.

V. CONCLUSION

Our work is focused on developing a tool to extend the period of independent living for PLWD. Following consultations with dementia specialists and a systematic literature review, we plan to incorporate ADLs, IADLs and MAs into a tool for PLWD. Monitoring performance of activities will be by sensors, where possible, or self-reported by app. Future work will focus on development of the combined app and activity detection via sensors.

ACKNOWLEDGMENT

This material is based on works supported by the Science Foundation Ireland under Grant No. 19/FFP/6917.

REFERENCES

[1] J. Turner, C. Nugent, D. Berry, J. Doyle, M. Wilson, and D. O'Sullivan, Individualised Self-Care for Early-Stage Dementia: A Framework for Activity Attainment and Replacement. International Journal On Advances in Life Sciences, vol. 14, 2022 (in press).

[2] S. Katz, A. B. Ford, R. W. Moskowitz, B. A. Jackson, and M. W. Jaffe, "Studies of illness in the aged. The Index of ADL: a standardized measure of biological and psychosocial function," JAMA, vol. 185, pp. 914-919, Sep. 1963, doi:10.1001/jama.1963.03060120024016.

[3] M. P. Lawton and E. M. Brody, "Assessment of older people: Self-maintaining and instrumental activities of daily living," The Gerontologist, vol. 9, pp. 179-186, 1969, doi:10.1093/geront/9.3_Part_1.179

[4] L. Teri and R. G. Logsdon, "Identifying pleasant activities for Alzheimer's disease patients: the pleasant events schedule-AD," The Gerontologist, vol. 31, pp. 124-7, Feb. 1991, doi:10.1093/GERONT/31.1.124

[5] American Psychiatric Association, Diagnostic and Statistical Manual of Mental Disorders, Fifth Edition (DSM-5), Arlington: American Psychiatric Association, 2013.

Covid-19: Comorbidities, Symptoms, and Hospitalization – a Review

Marisa Pires
Polytechnic Institute of Castelo Branco, Portugal
email: marisa.pires@hotmail.com

Filipe Fidalgo
R&D Unit in Digital Services, Applications and Content, Polytechnic Institute of Castelo Branco, Portugal
email: ffidalgo@ipcb.pt

Ângela Oliveira
R&D Unit in Digital Services, Applications and Content, Polytechnic Institute of Castelo Branco, Portugal
email: angelaoliveira@ipcb.pt

Abstract—**The increased number of daily Covid-19 infections in several countries around the world has proven to be a public health concern. To verify the association between comorbidities, hospitalizations, deaths, recoveries, symptoms, age and gender, this article investigates related studies in the databases "Medrxiv", "Google Scholar" and "Science Direct", with the following search terms "Covid-19 ", "Models", "Comorbidities", "Infection", "Hospitalization" and "Recovered". Thus, it was possible to verify that the most verified comorbidity is cardiovascular disease and that comorbidities together with Covid-19 infection are the main cause of hospitalization worldwide, prolonging the infection status that can lead to death. The analysis of the results allowed showing the indicators and trends, as well as the relationship between the variables that can assist in future decision making.**

Keywords- Covid-19; Comorbidity; Symptoms; Hospitalization; Age.

I. INTRODUCTION

Covid-19, also known coronavirus, emerged in December 2019 in the Chinese city of Wuhan. According to [1], everything indicates that the epicentre of the virus happened in a Wild Animal Market where there are birds, snakes, bats, and other animals. Coronavirus is a virus that causes respiratory infections in humans and animals whose name Covid-19 was reported by the "World Health Organization" (WHO) [2] and is the result of the fusion of the words "corona" and "virus", with the year it emerged, 2019 [3]. After exposure to the virus, infected humans begin to have the first symptoms in the first 2 to 14 days. The symptoms include dry and persistent cough, fever above 38ºC, excessive tiredness, generalized muscle pain, headache, sore throat, runny nose, or stuffy nose, diarrhea, loss of taste and smell [4]. There were also infected individuals who did not reveal symptoms, being asymptomatic. So far, the only way to know the presence of Covid-19 is by testing. Currently, there are 4 types of tests: molecular Nucleic Acid Amplification Tests (TAAN), also called Polymerase Chain Reaction (PCR), Rapid Antigen Tests (TRAg), Self-Testing and Serological Tests [5]. The most reliable and required by the authorities to travel are mainly PCR tests.

The first 14 days in which the human being was exposed to the virus are the days when contagion is greatest, isolation being therefore mandatory, since it is at this stage that the chains of contagion are created. After 14 days, the virus ceases to be transmitted and the human in question can end the isolation [6].

To prevent the spread of the virus, the National Health System (SNS) recommends specific prevention measures such as social distancing, the use of masks, frequent hand washing, disinfection, cleaning, and disinfection of spaces and recommends citizens to be aware of symptoms [7]. As there is still no direct treatment for Covid-19, the infected are medicated according to the symptoms presented with existing medications to reduce the fever and difficulty breathing. However, comorbidities may influence the severity of symptoms and infection [8]. Over months, it has also been verified that people with comorbidities are more prone to contracting the virus. This fact is reflected in regular hospitalizations and in intensive care units, where the number of deaths in these circumstances has increased.

Thus, a systematic study was carried out to identify associations between people infected with Covid-19 in ages, gender, symptoms, hospitalization, recoveries, and deaths, focusing on the associated comorbidities. This study corresponds to the first part of a more wide-ranging project to identify, in future work, the respective correlations and specific values for the measures/tests.

This article is divided into four sections. In Section I, we explain the methodology used and the article selection process. Section II contains the analysis of results and Section III the discussion of the results. Finally, in Section IV, the conclusions and further work are presented.

II. METHODOLOGY

Based on the PRISMA systematic review methodology [9] this article investigates related studies in the “Medrxiv”, “Google Scholar” and “Science Direct” databases with the following search terms "Covid-19", "Models", "Comorbidities ", "Infection", "Inpatient" and "Recovered".

Three reviewers independently assessed each study. The compliance was determined unanimously by all parties involved. The aim of this study was to verify the different methods of data analysis and models applied to the study and evolution of the mentioned terms. The search for articles was carried out between February and May 2021.

A. Research questions

The main research questions about this review were:

(Q1) Association between comorbidities and hospitalizations/deaths.
(Q2) Association between comorbidities and recoveries.
(Q3) Association between symptoms and hospitalization.
(Q4) Association between age, death, and gender.

B. Inclusion criteria

The inclusion criteria of studies and evaluation methods for this review were:

- Studies that aim to analyze pandemic data in various vacancies and in multiple countries of the world.
- Studies using machine learning and data processing to make predictions of the evolution of the pandemic.
- Studies that relate the numbers of Covid-19 infected people with hospitalizations and deaths.
- Studies that relate the numbers of Covid-19 infected people with comorbidities and recovered.
- Studies published between 2019 and 2021.

After the search using the referred terms, 263 articles were found, of which 42 were considered by application of the inclusion criteria. Figure 1 illustrates the resulting flowchart of feature extraction. During the study selection process, 11 repeated articles and 2 studies that were not in article format were initially removed. Then, 10 articles were removed because they did not fit the Covid-19 theme and finally 199 articles because they did not fit the research objective, although they addressed the Covid-19 theme. Of these 199 articles, 6 addressed climatic conditions and Covid-19, 2 the presence of Covid-19 in migrants, 141 study of the behaviour of other specific diseases in the presence of covid-19, 12 transmissibility factors, 23 socioeconomic factors and 15 hospital logistics. The remaining 42 studies were presented in the qualitative and quantitative synthesis. Data were extracted from all identified studies using a predefined format. Data extracted included: Study; Publication Year; Data Range Study; Methods; Comorbidity. Three reviewers extracted the information, and any disagreements were resolved via discussion. Table I identifies the extracted data and the characteristics of the included studies.

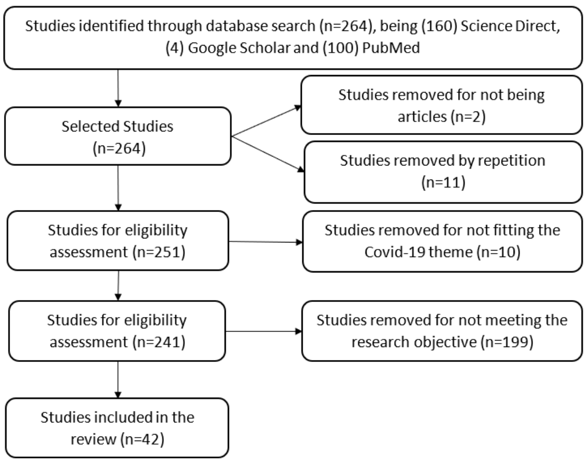

Figure 1 - Flow diagram for new systematic reviews (adapted from [9])

TABLE I . EXTRACTED DATA.

Study	***Data Range Study***	***Methods***	***Comorbidity***
[10]	February to June 2020	Machine Learning and Cox Regression Model	Neoplasm, diabetes, asthma, pulmonary, hepatic, hematological, renal, neurological, neuromuscular and immunodeficiency conditions
[11]	June 2020	Seaborn and SciPy	Asthma, malignancy, chronic hematological disorder, diabetes, HIV/other immunodeficiency, renal disease, liver disease, chronic lung disease, and neuromuscular disorder.
[12]	April 2020	Cohort and Poisson Regression	Comorbidities in general
[13]	February 2021	Developed a simple model	Type II diabetes, hypertension, cardiovascular disease, chronic kidney disease etc
[14]	April 2020	Empirical observation	Obesity in males, lung cancer death rates
[15]	November 2020	Review of literature published	HIV
[16]	NA	Methodology Mantegna	–
[17]	November 2020	Machine Learning	Medical condition
[18]	NA	Data-driven modelling MFTG	–
[19]	May 2020	Applied meta-analysis and meta-regression	–
[20]	June 2020	Spearman	Advanced age, obesity, cardiovascular disease, diabetes, and cancer
[21]	June 2020	Machine Learning algorithms	Comorbidities in general
[22]	May 2020	Developed the "Covid-19 trajectory viewer"	Comorbidities in general
[23]	March 2020	Meta-Analyses	Comorbidities in general
[24]	April 2020	Linear models regression	Comorbidities in general
[25]	First 14-16 weeks	Data extraction and analysis	–
[26]	February 2020	Monte Carlo simulation	Hypertension, diabetes, cardiovascular disease, chronic respiratory disease, and cancer
[27]	December 2019	Machine Learning	Comorbidities in general
[28]	May 2020	Developed a script program	Comorbidities in general
[29]	April 2020	Data processed with MS Excel	Comorbidities in general
[30]	NA	CFR	Comorbidities in general
[31]	April 2020	Random-effects and meta-analysis	Comorbidities in general
[32]	March to June 2020	Statistical analysis	Comorbidities in general
[33]	February to March 2020	Data processed with MS Excel	Comorbidities in general
[34]	December 2019 to October 2020	Aggregation data	Chronic respiratory illnesses, cardiovascular disease, hypertension, or diabetes mellitus

Study	***Data Range Study***	***Methods***	***Comorbidity***
[35]	January 2020	Random effects model	Cardiac, pulmonary, renal functions, and immunosuppressive states
[36]	NA	Mathematical model	–
[37]	NA	Meta-analysis	Hypertension, cardiovascular and cerebrovascular disease, and diabetes were
[38]	NA	Aggregation data	Comorbidities in general
[39]	14-16 weeks since the first death	Aggregation data	Pneumonia, cardiovascular disease combining ischaemic heart disease and stroke, chronic obstructive pulmonary disease, cancer, road traffic accidents and dementia
[40]	December 2020 and 24 April 2020	Statistical software package	Comorbidities in general
[41]	April 2020	Aggregation data	Comorbidities in general
[42]	December 2019 to April 2020	Stepwise forward regression	Diabetes, hypertension, chronic respiratory diseases, cancer, and cardiovascular disorders,
[43]	May 2020	Aggregation data	Comorbidities in general
[44]	May 2020	Aggregation data	Comorbidities in general
[45]	March 2020 until April 2020	Machine learning models	Comorbidities in general
[46]	NA	Aggregation data	Hypertension, type 2 diabetes, ischaemic heart disease, chronic obstructive pulmonary disease, cancer and overweight or obesity
[47]	March 2020	Exponential growth	Comorbidities in general
[48]	April 2020	Cohort	Chronic kidney disease
[49]	April 2020	Meta-analysis	Hypertension, diabetes, cardiovascular disease, lung disease, renal disease, cancer, and immunosuppression
[50]	June 2020	Meta-analysis	High blood pressure, diabetes mellitus, ischemic heart disease, and chronic obstructive pulmonary disease

III. DISCUSSION / RESULTS ANALYSIS

This work shows how the collection of daily data of people infected by Covid-19 is important, because it allows contributing to the knowledge and evolution of the pandemic and to understand how the new virus acts and propagates.

The research of the articles was conducted between February and May of 2021 in the databases "Medrxiv", "Google Scholar" and "Science Direct" and of which resulted 42 articles, 27 addressed data analysis, 7 article research, 5 " Machine Learning", 2 CFR Method and 1 Mathematical Model "Data-Driven MFTG", as illustrated in the graph in Figure 2.

Throughout the study, several data collection dates were verified, but still the data from the first wave were the ones that prevailed in most articles, even though some did not read this same information, as illustrated in the graph in Figure 3. In the articles studied, some methods of data analysis and tools were used, such as “Machine Learning” methods or a simple spreadsheet for statistical analysis. With these methods and tools, it is possible to draw several conclusions.

(**Q1**) Association between Comorbidities and Hospitalizations/Deaths: Comorbidities in conjunction with Covid-19 infection have been shown to be the leading cause of hospitalization, both in wards and in ICU’s [10][40]. These hospitalizations by Covid-19, where comorbidities are present were not only in Portugal [11], but in several countries of the world as referenced in [20]. As for the most frequently verified comorbidities, cardiovascular diseases [34][37][49] diabetes, hypertension, respiratory diseases, among others. Figure 4 shows comorbidities most frequently reported in the studies analyzed. It is [14] also evidenced that pre-existing diseases prolong the state of Covid-19 infection and that it can lead to death mainly in the older population. Age together with comorbidities showed an increase in the number of hospitalizations and the risk of death as reported in [25] where the most affected ages were between 80 and 89 years of age [12]**.** Similarly, in [29], it is reported that age was the main risk factor and that the virus mainly affected the elderly population, reinforced by [33]**,** however [23] reported that the median of the ages of the infected varied between 28 and 70 years.

(**Q2**) Association between Comorbidities and Recoveries: Recovery time was also shown to be influenced by comorbidities, because the more severe the comorbidity, the longer the recovery time [22]. Also, the data analysis [48] showed that the mean follow-up time of a patient infected by Covid-19 was 27 days and that the median age was 50 years, with the male gender being the most affected. However, many studies have not been found, which at this stage, addressed those recovered and their post-infection health status.

(**Q3**) Association between symptoms and hospitalization: Many Covid-19 infected patients were considered asymptomatic due to the absence of symptoms, however, many of the symptomatic patients had to be hospitalized due to their severity. In [15]**,** it was found that the diagnosis rate of Covid-19 was directly linked to the presence of symptoms and consequent hospitalization in the most severe cases, thus increasing the risk of mortality. Applications of data analysis and creation of illustrative graphs were also developed to assist in the treatment of Covid-19. The 'Covid-19 trajectory viewer' [22] generates graphs with data of recovered and dead as well as of the spread of the epidemic in the population through hospitalized versus not hospitalized, symptomatic versus asymptomatic, highly exposed versus less exposed professions.

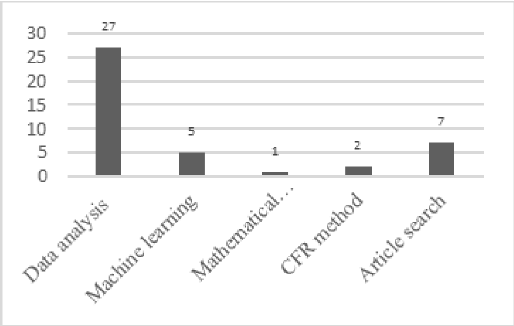

Figure 2 - Type of methods

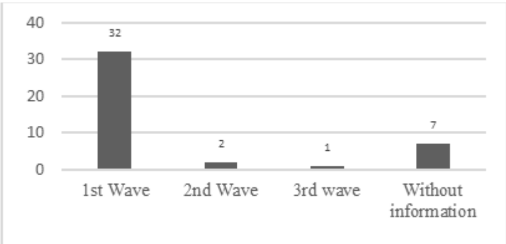

Figure 3 - Distribution of data by vacancy

(**Q4**) Association between age, death, and gender: As mentioned in Q1, the age and gender of the infected may vary considerably, but in [19], the authors found that men were more susceptible to death than women. Also in [26] [31] and [36], it is shown that patients over 60 and 70 years of age had a higher risk of contracting Covid-19, which was even higher than any comorbidity. The genus masculine was the one with the highest rate of infection referred to in [35] [39] [43]. In [41], it was found that individuals aged 80 years or older were responsible for most deaths in Europe. As for patients between 30 and 39 years of age, they had some immunity or resistance to the disease. In [34] and [51], it was found that patients with cardiac complications associated with SARS-CoV-2 were, on average, 10 years older than those who did not. The graph in Figure 5 was presented in [10] and is similar to the conclusions presented in [13], clearly showing that death from Covid-19 occurs in the older age groups and that in the younger age groups the number of deaths is practically nil.

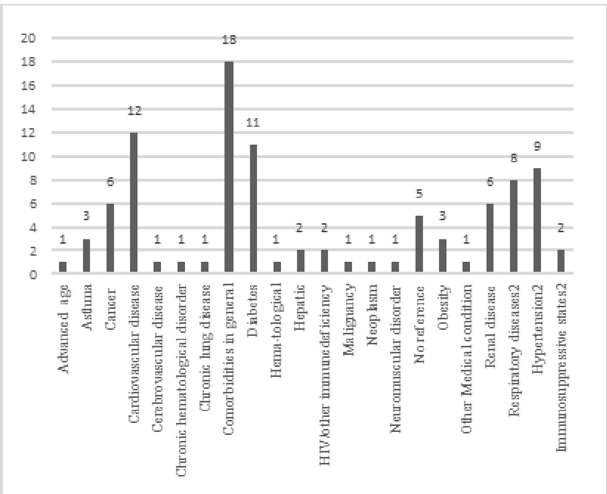

Figure 4 - Frequency of comorbidies

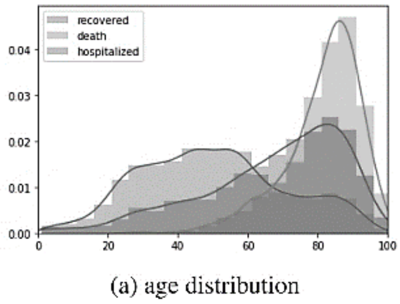

Figure 5 - Curve of ages most affected in the Covid infection-19 (adapted from [12])

IV. CONCLUSIONS

In December 2019, little was known about the virus called Covid-19 by the WHO, nor how to combat it. To avoid the rapid contagion seen in China, many countries have chosen to implement mandatory containment measures, mandatory use of masks on public roads and social distancing measures that later proved to have a major impact on transmission chains [16]. The way the virus operated by different infected patients was also a major object of study [18] [21], where not all infected had symptoms and others were so severely attacked that they had to be admitted to intensive care units and breath with the help of ventilators. As for symptoms, they varied from patient to patient depending on both the presence and the type of comorbidities. However, the comorbidity that stood out was cardiovascular disease followed by diabetes, hypertension, respiratory diseases, cancer, kidney diseases, asthma, obesity, immunosuppressive diseases, liver diseases, HIV, neuromuscular and cerebrovascular diseases, advanced age and other unspecified or unreported [34][37][49]. Comorbidities in conjunction with Covid-19 infection have also been found to be the leading cause of hospitalization worldwide [11] [20], prolonging the state of the infection that can lead to death. Recovery time was also shown to be influenced by comorbidities, where the more severe the comorbidity, the longer the recovery time [22], compared to the mean time of infection and recovery of 27 days [15][22][48]. Age, together with comorbidities, increased the number of hospitalizations and the risk of death, where the most affected ages were between 70 and 89 years [12] [25]. Still, in addition to comorbidities, the age group between 60 and 70 years of age also has a very high risk of contracting covid-19 infection [26] [31]. The number of deaths is strongly observed in males [19] and occurs in the older age groups [13]. In the younger age groups, the mean age of the infected varied between 28 and 70 years [41] and the number of associated deaths is very close to zero. Covid-19 has been shown to be present in virtually all age groups, but it is in the population over 60 years of age that infections are more severe. This population over 60 years of age revealed a higher presence of comorbidities, mainly cardiac and respiratory, which hinders recovery and, consequently, can lead to death.

In future work, in the next phase of this study, the available data sets will be combined with the statistical measures to quantify the respective values/metrics of correlations between the identified associations.

REFERENCES

[1] S. A. Ivan, "your money," 29 03 2020. [Online]. Available: https://www.seudinheiro.com/2020/colunistas/seu-mentor-de-investimentos/covid-19-como-tudo-comecou-ou-voce-esta-preparado-para-o-proximo-coronavirus/. [Accessed 11 12 2020].

[2] World Health Organization, [Online]. Available: https://www.who.int/emergencies/diseases/novel-coronavirus-2019. [Accessed 28 07 2022].

[3] B. U. Science, "UFABC Spread Science," 15 04 2020. [Online]. Available: https://ufabcdivulgaciencia.proec.ufabc.edu.br/2020/04/15/muitas-informacoes-sobre-o-novo-coronavirus-1-pra-comecar-covid-19-ou-sars-cov-2v-3-n-4-p-8-2020/. [Accessed 27 07 2022].

[4] D. S. Hinrichsen, "your health," 06 2021. [Online] Available: https://www.tuasaude.com/coronavirus/. [Accessed 07 07 2021].

[5] S. N. Saúde, (DGS), "SNS 24," 1 07 2021. [Online]. Available: https://www.sns24.gov.pt/guia/teste-covid-19/. [Accessed 07 07 2021].

[6] "SEPRI Group," 25 01 2021. [Online]. Available: https://www.sepri.pt/en/news/evolu%C3%A7ao-contagio-transmissao-covid19. [Accessed 07 07 2021].

[7] "SNS 24," 04 05 2021. [Online]. Available: https://www.sns24.gov.pt/tema/doencas-infecciosas/covid-19/prevencao/. [Accessed 07 07 2021].

[8] D. B. Clarisse, "Tua Saúde," 04 2021. [Online]. Available: https://www.tuasaude.com/tratamento-para-coronavirus-covid-19/. [Accessed 07 07 2021].

[9] M. J. Page et al., "PRISMA 2020 explanation and elaboration: Updated guidance and exemplars for reporting systematic reviews," pp. BMJ, vol. 372, Mar. 2021, doi: 10.1136/BMJ.N160, 07 05 2022.

[10] P. Andre, S. C. Rafael and H. Rui, "COVID-19 in Portugal: predictability of hospitalization, ICU and respiratory-assistance needs," doi: https://doi.org/10.1101/2020.09.29.20203141, 29 09 2020.

[11] F. Miguel et al., "Comparison of multimorbidity in covid-19 infected and general population in Portugal," doi: https://doi.org/10.1101/2020.07.02.20144378, 08 09 2020.

[12] R. P. Vasco et al., "COVID-19: Determinants of Hospitalization, ICU and Death among 20,293 reported cases in Portugal," doi: https://doi.org/10.1101/2020.05.29.20115824, 30 05 2020.

[13] A. Levi, P. Ashok and Z. Sammy, "The Longevity-Frailty Hypothesis: Evidence from COVID-19 Death Rates in Europe," doi: https://doi.org/10.3390/ijerph19042434, 23 02 2021.

[14] N. Alessio and T. Giorgio, "COVID-19 transmission risk factors," COVID-19 transmission risk factors, doi: 10.1080/20477724.2021.1993676, 12 05 2020.

[15] D. M. Elnara, "Does HIV impact susceptibility to COVID-19 (SARS-CoV-2) infection and pathology? A review of the current literature," doi: https://doi.org/10.1101/2020.12.04.20240218 , 07 12 2020.

[16] G. B. Juan et al., "Analysis of communities of countries with similar dynamics of the COVID-19pandemic evolution," doi: https://doi.org/10.1101/2021.01.18.21250050, 20 01 2021.

[17] R. José and P. G. Carlos, "Comparing Decision Tree-Based Ensemble Machine Learning Models for COVID-19 Death Probability Profiling," doi: https://doi.org/10.1101/2020.12.06.20244756, 8 12 2020.

[18] T. Hamidou, "COVID-19: Data-Driven Mean-Field-Type Game Perspective," COVID-19: doi. https://doi.org/10.1101/2020.07.23.20160853, 25 07 2020.

[19] P. M. Thaise, A. S. Delvan and N. B. Alexandre "Are men dying more than women by COVID-19? Running Title: COVID-19 prevalence by gender in the world," doi: https://doi.org/10.1101/2020.07.06.20147629, 07 07 2020.

[20] O. Ouail and D. B. Asmaa, "Risk Factors for Mortality of COVID-19 Patients," doi: https://doi.org/10.1101/2020.07.02.20145375 , 07 07 2020.

[21] V. Adriano and Z. Nivio, "Explainable death toll motion modeling: COVID-19 narratives and counterfactuals,"doi: 10.1371/journal.pone.0264893, 06 07 2020.

[22] L. W. Loeffler, S, Maria and B. Hans, "Covid-19 trajectories – Monitoring pandemic in the worldwide context," doi: https://doi.org/10.3390/v12070777, 5 06 2020.

[23] D. F. Santos, P. Maranhão and M. S. Monteiro, "Identifying baseline clinical features of people with COVID-19," doi: https://doi.org/10.1101/2020.05.13.20100271, 16 05 2020.

[24] R. R. Witold and P. Radoslaw, "Estimate of Covid prevalence using imperfect data," doi: https://doi.org/10.1101/2020.04.14.20064840, 17 04 2020.

[25] O. Bayanne et al., "Population perspective comparing COVID-19 to all and common causes of death in seven European countries," doi: https://doi.org/10.1101/2020.08.07.20170225 , 11 08 2020.

[26] C. Francisco, F. Nuno and O. Barbara, "Estimation of risk factors for COVID-19 mortality -preliminary results," doi: https://doi.org/10.1371/journal.pone.0247461, 25 02 2020.

[27] T. H. Abaker et al., "A Machine Learning Solution Framework for Combatting COVID-19in Smart Cities from Multiple Dimensions," doi: https://doi.org/10.1101/2020.05.18.20105577 , 14 06 2020.

[28] M. O. Rogelio and V. A. Damián, "The misleading illusion of COVID-19 confirmed case data: alternative estimates and a monitoring tool," doi: https://doi.org/10.1101/2020.05.20.20107516, 25 05 2020.

[29] P. G. Hui et al., "Risk factors affecting COVID-19 case fatality rate: A quantitative analysis of top 50 affected countries," doi: https://doi.org/10.1101/2020.05.20.20108449 , 25 05 2020.

[30] C. Martí et al., "Robust estimation of diagnostic rate and real incidence of COVID-19 for European policymakers," doi: https://doi.org/10.1371/journal.pone.0243701 , 05 06 2020.

[31] F. C. Jérémie et al., "COVID-19-related doi: https://doi.org/10.1101/2020.04.11.20061721, 16 04 2020.

[32] G. Valentina et al., "1 Comparing the COVID-19 pandemic in space and over time in Europe, using numbers of deaths, crude rates and adjusted mortality trend ratios,"doi: https://doi.org/10.1038/s41598-021-95658-4, 24 08 2020.

[33] K. M. Wittkowski, "The first three months of the COVID-19 epidemic: Epidemiological evidence for two separate strains of SARS-CoV-2 viruses spreading and implications for prevention strategies," doi: https://doi.org/10.1101/2020.03.28.20036715, 29 04 2020.

[34] E. S. Jane et al., "A meta-analysis on the role of pre-existing chronic disease in the cardiac complications of SARS-CoV-2 infection," doi: https://doi.org/10.1101/2020.06.21.20136622, 5 03 2021.

[35] P. L. Swaminathan et al., "Higher mortality in men from COVID19infection-understanding the factors that drive the differences between the biological sexes," doi: https://doi.org/10.1101/2020.04.19.20062174, 19 04 2020.

[36] H. A. Houssein et al., "Age could be driving variable SARS-CoV-2 epidemictrajectories worldwide," doi: https://doi.org/10.1371/journal.pone.0237959, 17 04 2020.

[37] T. Rogério, S. Mário and G. Victor, "COVID-19 and cardiovascular comorbidities: An update," doi: https://doi.org/10.1016/j.repc.2020.06.013, 9 07 2020.

[38] M. Aguiar and N. Stollenwerk, "Condition-specific mortality risk can explain differences in COVID-19case fatality ratios around the globe," doi: https://doi.org/10.1016/j.puhe.2020.08.021, 6 09 2020.

[39] O. Bayanne et al., "Population perspective comparing COVID-19 to all and common causes of death during the first wave of the pandemic in seven European countries," doi: 10.1016/j.puhip.2021.100077 , 15 01 2021.

[40] M. D. Ana, G. M. Nilza and F. M. Cláudia, “COVID-19 fatality rates in hospitalized patients: systematic review and meta-analysis,” doi: https://doi.org/10.1016/j.annepidem.2021.02.012, 02 03 2021.

[41] P. I. John, A. Cathrine and G. C. Despia, “Population-level COVID-19 mortality risk for non-elderly individuals overall and for non-elderly individuals without underlying diseases in pandemic epicenters,” doi: https://doi.org/10.1101/2020.04.05.20054361, 1 07 2020.

[42] S. Srikanta et al., “Examining the association between socio-demographic composition and COVID-19 fatalities in the European region using spatial regression approach,” doi: https://doi.org/10.1016/j.scs.2020.102418, 1 08 2020.

[43] R. Serge, V. Jean and M. Charlotee, “Are we equal in adversity? Does Covid-19 affect women and men differently?,”doi: https://doi.org/10.1016/j.maturitas.2020.05.009, 15 05 2020.

[44] K. V. Henu et al., “Current updates on the European and WHO registered clinical trials of coronavirus disease 2019 (COVID-19),” doi: https://doi.org/10.1016/j.bj.2020.07.008, 24 07 2020.

[45] A. Alhanoof et al., “Prediction of COVID-19 Individual Susceptibility using Demographic Data: A Case Study on Saudi Arabia,” doi: https://doi.org/10.1016/j.procs.2020.10.051, 11 11 2020.

[46] P. K. Hans et al., “Prevention and control of non-communicable diseases in the COVID-19 response,” doi: https://doi.org/10.1016/S0140-6736(20)31067-9, 10 05 2020.

[47] O. K. Kin et al., “Herd immunity – estimating the level required to halt the COVID-19 epidemics in affected countries,” doi: https://doi.org/10.1016/j.jinf.2020.03.027, 21 03 2020.

[48] F. Pedro, V. Rita and S. C. Filipe, “Chronic kidney disease is associated with worse outcomes following SARS-CoV2 infection among 18647 patients: A population-based cohort study,” doi: 10.1016/j.nefro.2020.11.004, 16 02 2021.

[49] C. S. Silvia et al., “Coronavirus (SARS-CoV-2) and the risk of obesity for critically illness and ICU admitted: Meta-analysis of the epidemiological evidence,” doi: https://doi.org/10.1016/j.orcp.2020.07.007, 3 08 2020.

[50] V. B. Walter et al., “A review of the main histopathological findings in coronavirus disease 2019,” doi: https://doi.org/10.1016/j.humpath.2020.07.023, 2 08 2020.

[51] E. S. Jane et al., “A meta-analysis on the role of pre-existing chronic disease in the cardiac complications of SARS-CoV-2 infection,” doi: https://doi.org/10.1016/j.isci.2021.102264, 10 12 2020.

Estimation of Ground Reaction Force Using Wearable Sensors for Mobile Running Monitoring System

Kyoko Shibata, Shota Yagi, Yoshio Inoue
Kochi University of Technology
Tosayamada, Kami, Kochi, 782-8502, Japan
e-mail: shibata.kyoko@kochi-tech.ac.jp, yagishota_kut@yahoo.co.jp, inoue.yoshio@kochi-tech.ac.jp

***Abstract*— Many people run to maintain or improve their health. If we can monitor our own form during daily running, it is useful in designing our own health promotion for effective exercise. The ground reaction force is a way of quantitatively evaluating a running form. Therefore, to obtain ground reaction force as health information with light burden to runners, this study will develop a wearable estimation method of ground reaction force. So far, we have established a method during walking using 15 inertial measurement units. Therefore, this report applies it and estimates ground reaction forces in two directions while running. Furthermore, we propose to reduce the number of sensors to 5 using correlation between accelerations so that the runner can more easily perform the measurements. The estimated values by each proposed method are compared with the measured values. The results showed that the high accuracy of the vertical ground reaction force was maintained after the reduction, but in the anterior-posterior direction, the high accuracy was not achieved.**

Keywords-health promotion; inertial measurement unit; correlation coefficient; force plate; inertial force.

I. INTRODUCTION

One of the sports to promote health is jogging and running. Due to its simplicity, about 10% of the population in Japan practices it [1]. In addition, many wearable devices (such as smart watches) that record running motion are commercially available. Many of these provide data such as distance, average speed, altitude differences, calories, and so on. If the running activity is performed using correct form, a beneficial effect for health can be expected; however, if an incorrect form is used, it may cause damage to the knees and foot soles. However, a simple smart watch cannot easily monitor a person's running form.

The Ground Reaction Force (GRF) is a way of quantitatively evaluating a form [2]. The magnitude and phase of GRF can indicate the quality of the form. Conventionally, GRF is measured by using an installation type or sole mounting type force plate, which is expensive, causes an uncomfortable form, and cannot measure a long distance. Therefore, this study develops a wearable system that can easily monitor GRF during daily running. Obtaining GRF, which can assess running form, as a one of health information could be useful in designing one's own health promotion for effective exercise.

So far, we have proposed a method to estimate GRF during walking without using Force Plate (FP) [3]. In this estimation system, the whole body is divided into 15 parts. The inertial force of each part is derived from the dynamic acceleration measured by Inertial Measurement Unit (IMU) attached to each part. In the vertical direction, the sum of the inertial force of each part and the gravity balances GRF, so that GRF during walking can be estimated. Similarly, in the anterior-posterior direction, the sum of the inertial forces of the respective parts balances GRF.

There are three major differences between running and walking. First, running is a faster movement, so the acceleration is large and the impact force is large. Second, when running, there is no two-leg support period. Third, there is a period when neither foot is on the ground (referred to as the "aerial period" in this report). Thus, in this report, we experimentally examine whether the estimation method for walking with IMUs described above can be applied to running. At this time, the GRF is corrected for the aerial phase. Furthermore, we propose to reduce the number of sensors mounting positions from 15 to 5 using the correlation so that the runner can more easily perform the measurements. In addition, the accuracy in estimation is examined. In this estimation, the vertical and the anterior-posterior directions are targeted. Section II describes an estimating method for GRFs and running experiments. Section III proposes a method to reduce the number of sensors and confirms the accuracy from experimental results. Finally, Section IV presents the conclusions.

II. ESTIMATION OF GRFS DURING RUNNING

In this study, the whole body is divided into the 15 parts shown in Table 1, referring to the work by Ae et al. [4]. An inertial force of each part is derived from a mass of each part m_i and each dynamic acceleration a_i, and when these are added, the total inertial force of the whole body is obtained. The sum of the total inertial force and the gravity balances the vertical GRF. If the whole body mass is M, then the vertical GRF F_z can be expressed by (1).

$$F_z = \sum_{i=1}^{15} m_i a_i + Mg \quad (1)$$

Here, m_i can be derived by multiplying M by each body mass ratio [4] R_i in Table 1.

Using vertical dynamic accelerations measured by IMUs,

TABLE I. PHYSICAL INFORMATION [4] AND PARAMETER NOTATION

Body part(s)	Mass ratio (one side)	Parameter notation	
		Mass ratio	Acceleration
Head	0.069	R_{hd}	a_{hd}
Upper trunk	0.302	R_{ut}	a_{ut}
Lower trunk	0.187	R_{lt}	a_{lt}
Upper arm (x2)	0.027	R_{ua}	a_{ua}
Forearm (x2)	0.016	R_{fa}	a_{fa}
Hand (x2)	0.006	R_{hn}	a_{hn}
Thigh (x2)	0.110	R_{th}	a_{th}
Shank (x2)	0.051	R_{sh}	a_{sh}
Foot (x2)	0.011	R_{ft}	a_{ft}

the vertical GRF F_z can be estimated by the (2). Here, as shown in Table 1, the mass ratio and the acceleration of each part are indicated by subscripts. In addition, for the accelerations of the left and right parts, the subscripts "l" and "r" are further added to each. Furthermore, the last subscript "z" indicates the vertical direction (e.g., the vertical acceleration of the right upper arm is shown as a_{uarz}, and the left one is shown as a_{ualz}).

$$\begin{aligned} F_z = (&R_{hd}a_{hdz} + R_{ut}a_{utz} + R_{lt}a_{ltz} + R_{ua}a_{uarz} + R_{ua}a_{ualz} \\ &+R_{fa}a_{farz} + R_{fa}a_{falz} + R_{hn}a_{hnrz} + R_{hn}a_{hnlz} + R_{th}a_{thrz} \\ &+R_{th}a_{thlz} + R_{sh}a_{sharz} + R_{sh}a_{shlz} + R_{ft}a_{ftrz} + R_{ft}a_{ftlz})M + Mg \end{aligned} \quad (2)$$

Furthermore, the anterior-posterior GRF is derived by removing the gravitational term and replacing the vertical acceleration with the anterior-posterior acceleration, in (2).

To examine the accuracy of this proposed method, running experiments are performed. Three healthy Japanese male volunteers (Age: 21.3±0.7, Height: 1.69±0.03[m], Weight: 68.3±0.2[kg]) participated. This experiment is approved by the Kochi University of Technology Ethics Review Committee.

In the experiments, 15 IMUs (MTw2, Xsens), a Motion Capture (MC, MAC3D, Motion Analysis) for obtaining the true value of acceleration, and three FPs (one TF-6090 and two TF-4060, Tec Gihan) for obtaining the true value of GRF are used. Each IMU is attached to the center of mass [4] of the 15 body parts shown in Table 1, and a marker for MC is attached on IMU (Figure 1). Three free-running measurements per subject. The sampling frequency is 100[Hz], and the cutoff frequency of the low pass filter for smoothing is 9[Hz]. The comparison target is the 5th to 7th step on the FPs.

By substituting accelerations measured by IMUs and MC into (2), the GRFs in the vertical and anterior-posterior directions are derived. Furthermore, the GRFs during the aerial period are corrected. The reason for the correction is that the inertia forces calculated from the body part acceleration are not zero because each body part is moving even during the aerial period. In other words, the GRFs derived from the accelerations during the aerial period are not zero. Therefore, the aerial period is estimated based on the vertical dynamic acceleration of the upper trunk, and only the GRFs during the aerial period is corrected to zero.

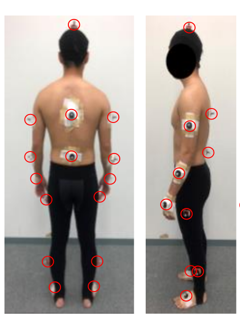

Figure 1. Positions where IMUs and MC markers are attached

The experimental results for one trial of one subject are shown. Other trials have obtained similar results. Figure 2 shows the GRFs estimated from IMUs (blue) or MC (orange) and measured by FPs (gray).

In the vertical GRFs shown in Figure 2(a), the estimated waveforms obtained by MC and IMUs matched very well with the FPs as the true value. The Mean Absolute Error (MAE) with the true value was 127.4 [N] for IMU and 96.0[N] for MC. The correlation coefficient was 0.943 for IMU and 0.953 for MC. However, the spike wave immediately after grounding that appears at FP could not be detected at IMU and MC. On the other hand, the anterior-posterior GRF in Figure 2(b) showed a difference in peak magnitude compared to FPs value for both MC and IMUs. In addition, phase differences also occurred in the estimated values. In the anterior-posterior direction, the MAE with the true value was 42.1[N] for IMU and 34.6[N] for MC. The correlation coefficient was 0.842 for IMU and 0.848 for MC. So, it was found that the accuracy in the anterior-posterior direction was lower than in the vertical direction. Moreover, although we were concerned about a loss of accuracy in the acceleration measurement with the IMU, in this case, the two estimated GRF methods by IMU or MC had almost waveforms, and errors introduced by the IMUs were not a problem.

III. REDUCTION OF THE NUMBER OF MEASURED PARTS

Section II estimated GRFs using the accelerations of all 15 parts of the body. This section proposes to reduce the number of parts to be measured, that is, the number of IMUs, to simplify the measurement.

In the proposed reduction method, when the acceleration values of multiple parts show similar tendency, a representative part is selected, and the acceleration of the representative part replaces the acceleration of the remaining parts. In other words, only accelerations of the representative parts are used to estimate GRFs, thereby reducing the number of measurement points.

A specific method is described. First, the acceleration values measured in the previous experiment are classified into the following three groups with similar tendency.

(A) Head, Upper trunk, Lower trunk
(B) Upper arm, Forearm, Hand
(C) Thigh, Shank, Foot

In fact, the total number of groups is 10, since each group is classified for each direction and for each side. Next, an equivalent acceleration is derived for each group. The equivalent acceleration is obtained by dividing the sum of the inertial forces of the considered parts by the sum of the considered parts masses. For example, the equivalent acceleration of group A in the vertical direction a'_{eqAz} is obtained by

$$a'_{eqAz} = (R_{hd}a_{hdz} + R_{ut}a_{utz} + R_{lt}a_{ltz}) / (R_{hd} + R_{ut} + R_{lt}) \cdot \quad (3)$$

Subsequently, using the measured values of the previous experiment, the equivalent acceleration is compared with the acceleration of each part in the group based on the correlation coefficient. As an example, Table 2 shows the results of group A in the vertical direction. From Table 2, the upper trunk with the highest correlation is selected as the representative part. In this way, representative parts are determined for each of the remaining 9 groups. As results, in this study, the five representative parts in the vertical direction were the upper trunk, right and left forearms, and right and left thighs. On the other hand, the five representative parts in the anterior-posterior direction were the upper trunk, right and left forearms, and right and left shanks.

Hence, for example, the vertical GRF F_{r_z} using only the representative part accelerations can be estimated by

$$F_{r\_z} = \{(R_{hd} + R_{ut} + R_{lt})a_{utz} + (R_{ua} + R_{fa} + R_{hn})(a_{farz} + a_{falz}) + (R_{th} + R_{sh} + R_{ft})(a_{thrz} + a_{thlz})\}M + Mg. \quad (4)$$

The results of the same trial as in Section II, with this proposed reduction method and correction in the aerial period, are shown. Figure 3 shows GRFs obtained from the five accelerations measured by IMUs or MC, and from FPs.

In the vertical GRF shown in Figure 3(a), no spike wave could be detected as before the reduction (Figure 2(a)). In addition, the waveforms near the peak values of the right foot (5th and 7th steps) were collapsed and the phase also differed. The MAE with the output value of FP as the true value was 142.7[N] for IMU and 147.6[N] for MC. The correlation coefficient was 0.928 for IMU and 0.925 for MC. However, generally similar tendency could be read for both IMU and MC, and there was no difference in the peak value from the true value. Furthermore, it is noteworthy that the estimated GRFs by IMU and by MC agree well, as they did before the reduction. Therefore, the accuracy of vertical acceleration measurements using the IMU was good. On the other hand, for the anterior-posterior GRF in Figure 3(b), although the general shapes were somewhat similar, both the waveform, peak value, and phase differed from the true value. The MAE with the true value was 55.6[N] for IMU and 55.6[N] for MC. The correlation coefficient was 0.693 for IMU and 0.765 for MC.

Moreover, the effect of reducing the number of sensors from 15 to 5 is discussed. For the vertical direction, from Figures 2(a) and 3(a), there is some error in the waveform after the peak value, but the reduction in accuracy is small. For the anterior-posterior direction, from Figures 2(b) and 3(b), the timing of the increase/decrease is the same, but errors occur, especially in positive magnitude.

TABLE II. THE CORRELATION COEFFICIENT OF VERTICAL ACCELERATIONS IN GROUP A.

Body part	Head	Upper trunk	Lower trunk
Correlation coefficient	0.978	0.989	0.986

IV. CONCLUSION AND FUTURE WORK

In this study, an estimation method used for the walking motion was applied to the running motion to estimate GRFs using wearable IMUs. As results, it was confirmed that the vertical GRF value estimated from the accelerations measured by the IMUs matched the measured FP value with good accuracy. However, due to the limitation of the sampling frequency of the IMU used, the spike wave immediately after grounding could not be obtained in this report. Since the IMU with a sampling frequency of 100[Hz] was used in this experiment, this problem could be solved by using a sensor that can measure at a sampling frequency of 200[Hz] or higher. On the other hand, the estimated anterior-posterior GRF value has low accuracy. Since the anterior-posterior acceleration values are small, the rotational misalignment of IMU during running has a significant effect on the estimation accuracy. The results using MC were estimated closer to FP than using IMU. Therefore, we believe that IMU mounting method needs to be improved. Moreover, we proposed a method of reducing the number of sensors using equivalent acceleration and correlation coefficients. In the vertical direction, the estimated GRF after the reduction was slightly less accurate than before the reduction but was almost the same as the measured value. In other words, the proposed reduction method maintained high accuracy. On the other hand, in the anterior-posterior GRF, the accuracy was further reduced compared to that before the reduction. In addition, the phase shift became larger. This result also suggests that one factor in the low accuracy is the misalignment of IMU. Furthermore, another factor was that representative body parts were selected based only on the correlation coefficient of acceleration, and we would like to consider adding the characteristic points of the waveform in the future. One factor was that representative body parts were selected based only on the correlation coefficient of acceleration, and we would like to consider adding the characteristic points of the waveform in the future. From the above, we have established a wearable estimation method for vertical GRF during running that reduces the burden on runners.

In the future, to improve the estimation accuracy of the two-directional GRF, we will consider the selection of appropriate sensor system and mounting methods and the introduction of frequency analysis to capture the characteristics of the waveforms, as described above. In parallel with these, we will explore the applicability of the proposed method to motions with higher running speeds. Furthermore, we will attempt long-distance running with IMUs, although this report we only measured two steps for verification purposes. In this case, we consider using a Kalman filter to compensate for the drift error, which is generally a problem for long-time measurements in IMU.

ACKNOWLEDGMENTS

Thanks to Mr. Shoya Fukumoto, a graduate of our laboratory, for his support. This work was supported by JSPS KAKENHI Grant Number JP18K11106.

REFERENCES

[1] https://www.ssf.or.jp/research/sldata/tabid/381/Default.aspx 2022/6/7. (in Japanese).

[2] J. B. Morley, L. M. Decker, T. Dierks, D. Blanke, J. French, and N. Stergiou, "Effects of varying amounts of pronation on the mediolateral ground reaction forces during barefoot versus shod running," J. of Applied Biomechanics, Vol. 26, Issue 2, pp. 205-214, 2010.

[3] A. Isshiki, Y. Inoue, K. Shibata, and M. Sonobe, "Estimation of floor reaction force during walking using physical inertial force by wireless motion sensor," HCI Intl. 2017, pp. 249-254, 2017.

[4] M. Ae, H. Tang, and T. Yokoi, "Estimation of inertia properties of the body segments in Japanese athletes," Soc. Biomechanisms Japan, 11, pp. 22-33, 1992. (in Japanese).

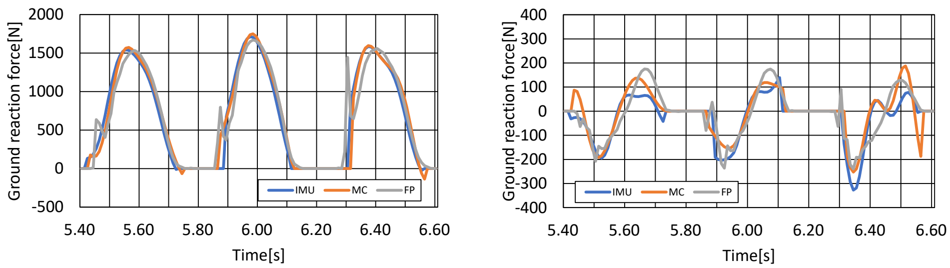

(a)The vertical direction.

(b) The anterior-posterior direction.

Figure 2. The GRFs estimated using 15 IMUs or MC. Here the GRF during the aerial period are corrected.

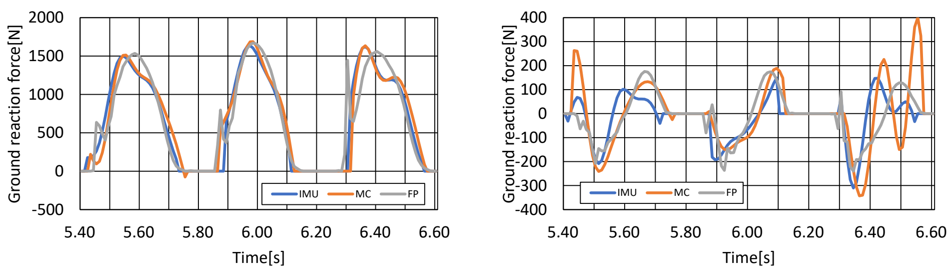

(a)The vertical direction.

(b) The anterior-posterior direction.

Figure 3. The GRFs estimated using 5 IMUs or MC. Here the GRF during the aerial period are corrected.

Analysis of Upper Limb Contraction Pattern Using Electromyographic Signal during Activities of Daily Living: a Pilot Study

Patrícia Santos
Physics Department, LIBPhys, NOVA School of Science and Technology, NOVA University of Lisbon
2829-516 Caparica, Portugal
Superior School of Health of Polytechnic Institute of Beja
7800-111Beja, Portugal
patricia.santos@campus.fct.unl.pt

Inês Garcia
Physics Department, NOVA School of Science and Technology, NOVA University of Lisbon
2829-516 Caparica, Portugal
ii.garcia@campus.fct.unl.pt

Cláudia Quaresma
Physics Department, LIBPhys, NOVA School of Science and Technology, NOVA University of Lisbon
2829-516 Caparica, Portugal
c.quaresma@fct.campus.unl.pt

Carla Quintão
Physics Department, LIBPhys, NOVA School of Science and Technology, NOVA University of Lisbon
2829-516 Caparica, Portugal
cmquintao@fct.unl.pt

***Abstract*— The upper limb is extremely important in the performance of Activities of Daily Living (ADLs), and its function is highly compromised when considering the sequelae of neuromotor diseases. It is essential to obtain more accurate information about the contraction patterns of the upper limb in healthy individuals, for a better understanding and assessment of the movements performed during ADLs in pathological situations, since conventional assessment methods do not provide objective data on the patient's performance. The integration of technological devices in the assessment of the contraction pattern will be an asset in obtaining more accurate information to expand our ability to know, predict and diagnose health conditions. A pilot study was conducted to characterize upper limb neuromotor biosignals during five ADLs in 18 healthy individuals. The BiosignalsPlux device was used to monitor the contraction pattern of the shoulder muscles by means of electromyography (EMG). Thus, the main objective of this article is to describe the results of the application of an experimental protocol to analyze the contraction pattern of six shoulder muscles during ADLs, through the electromyographic signal. Through this study, differences were verified in the patterns of muscle activation amplitude between ADLs directed to the midline, between ADLs directed to the contralateral side, as well as between these two groups of activities.**

Keywords- upper limb; electromyography; technology, activities of daily living, biomechanics.

I. INTRODUCTION

The performance and participation in Activities of Daily Living (ADLs) are strongly affected by the limitation of functional movements of the upper limb [1]. Functional use of the upper limb is highly compromised when considering stroke sequelae [2]. It is estimated that this affects about 80% of acute patients and 40% of chronic patients after stroke [3].

Upper limb paresis after stroke is characterized by decreased muscle strength [4] and loss of autonomy in ADLs [5]. About 37%-55% of subjects with stroke have deficits in the performance of these activities [6]. These deficits in the performance are related to the omission of small actions, changes in the sequence and in the quality of their performance, as demonstrated in studies related to the preparation of meals [7] and hygiene [8].

Impairment and disability in clinical settings are generally assessed by ordinal scales that are not very sensitive to the smallest and most specific changes [9]. More objective assessment methods are needed to evaluate and describe the upper limb function in detail [10].

An important factor for a better understanding and assessment of movements performed during ADLs, in pathological situations, is to understand the characteristics of the contraction patterns of the upper limb in healthy individuals in these same activities. The integration of technological devices that make it possible to obtain more accurate data about the contraction patterns in healthy subjects is extremely important here, since the expansion of knowledge about the contraction pattern in ADLs is only achieved through this type of information, so that later, in pathological conditions, we can predict and diagnose the changes more objectively.

A. *Data analysis of upper limb movement in ADLs*

Several studies have been performed using technology to study upper limb performance during functional tasks related to ADLs [10]-[16]. Although these studies are directed to the analysis of upper limb functionality, most of them focus on the study of kinetic and kinematic parameters and not on biosignals. Mainly using only technological tools such as optoelectronic motion analysis systems and inertial measurement sensors (3D accelerometer, 3D magnetometer and 3D gyroscope) [10]-[12][14][15]. However, they focus their analysis only on the performance of the activity, drinking from a glass [10]-[13][15] and only two of them analyzed the pattern of contraction of the muscles of the upper limb in ADLs [13][16], using surface electromyography (EMG).

Although kinematic analysis and kinetic analysis provide us with very relevant information in movement analysis, only through EMG can we know the amplitude of muscle activation of a group of muscles involved in ADLs.

EMG is the measurement of the electrical signal associated with muscle activity. Muscle excitation is then analyzed through the amplitude of the EMG signals, which means that the more motor units are recruited and the higher the firing rates, the greater the contraction by the muscle [17]. Through the EMG signal, muscle contraction and relaxation data are obtained, indicating whether the muscle is actively participating in the execution of the movement.

B. *Analysis of the muscle activation amplitude of the upper limb in ADLs*

According to one of the studies found [13], the sequence of muscle activation amplitude in the activity of drinking water from a glass, differs between subjects with and without stroke, regarding shoulder and arm muscles. In shoulder muscles, Superior Trapezius is activated throughout the activity, contrary to healthy subjects, who only activate in the phases of taking the glass to the mouth and returning to the table. The deltoids (anterior, middle, and posterior) in individuals with stroke are activated in the phases of "initial position to reach", "reach for the cup", "carry to mouth", while the control group only activates the anterior deltoid in the two first phases, the middle deltoid in the third phase and the posterior deltoid in the "return to pick up point" and "return hand to initial position".

In the study that our team developed previously [16] but in only one healthy individual, the results are indicative of differences in the pattern of activation amplitude between ADLs directed to the midline (drinking from a cup, eating soup and brushing teeth), between ADLs directed to the contralateral side (brushing the hair on the contralateral side of the head and washing the contralateral upper limb), as well as between these two groups of activities. In this study, two parameters were used to characterize the pattern of muscle contraction, the maximum peak of contraction amplitude (mV), that is, the maximum contraction amplitude verified in each of the muscles, as well as the time (s) in which these same maximums occur during the ADLs performance, which makes it possible to perceive the sequence of maximum amplitude of contraction activation of each muscle during the activity.

To better understand and evaluate the compensatory motor strategies developed by patients with neuromotor disorders, such as stroke, and to verify an inadequate pattern of muscle activation during ADLs, it is necessary to know the normal pattern of muscle activation in these activities, in healthy individuals. These compensatory motor strategies are very common in stroke patients and can cause severe musculoskeletal disorders, worsening the functional status of patients [18]. Therefore, it is essential that these compensatory patterns are detected early, thus preventing the installation of other types of dysfunctions resulting from stroke.

Biosignals give thus valuable information that provides a better perception of the patient's clinical status, constituting an important tool for clinical decision-making and measurement of the evolution resulting from clinical intervention [19].

The issue of this investigation focuses on exploring the applicability of the protocol [16] and characterizing the muscle activation pattern in healthy individuals in ADLs. This study aims to analyze and explore the characteristics (amplitude and sequence of muscle activation peaks) of the activation pattern of the electromyographic activity of the shoulder main muscles [20] during ADLs (eating, drinking, dressing and personal care) [21] in healthy individuals.

This article describes in Section 2, the materials, and methods (participants, equipment, and the experimental procedure of the investigation), in Section 3 the results, in Section 5, the discussion of them from a critical perspective and in Section 6 the main conclusions and perspectives.

II. Materials and Methods

This study was previously approved by the Ethics Committee and the Board of Directors of NOVA School of Science and Technology at NOVA University of Lisbon, and data collection was carried out at the same university.

A. *Characterization of the Sample*

This protocol was applied to 24 healthy adult subjects, selected for convenience. Of these individuals, 6 were excluded due to failure to capture the EMG signal during activities, leaving the sample with n=18 individuals. As exclusion criteria, diagnosis of neuromotor, cognitive or language deficits and changes in visual acuity not compensated by glasses or contact lenses were defined. The volunteer joined the study after reading and signing the informed consent.

The 18 participants who make up the sample of this study present the following characteristics: mean age of 29.1 years ± 3.2 in a range 19-62 years, in which 6 men and 12 women, 17 were dominant right-handers.

B. *Instruments*

To collect the EMG signals, the Biosignalsplux device was used, wirelessly connected to the OpenSignals (r)evolution software, for data acquisition, visualization, and processing, being a specific software for PLUX biosignal hardware platforms [22]. 6 channels were used to record bipolar EMG related to 6 different muscles and the signal was collected at a sample frequency of 1000Hz. [13].

The electrodes were placed 2 cm apart [23], according to the agonist muscles of the main shoulder movements namely the Pectoralis Major (PM), Anterior Deltoid (AD), Middle Deltoid (MD), Posterior Deltoid (PD), Upper Trapezius (UT) and Lower Trapezius (LT), responsible for flexion (F), extension (E), abduction (ABD), adduction (AD), scapular elevation (SE), and scapular depression (SD) [19].

C. *Experimetal Procedure*

The procedures for carrying out this study consisted of:

- Participants first performed activities directed to the midline (drinking from a cup, having soup, brushing teeth) and then to the contralateral side (brushing hair and washing the contralateral side), with the dominant limb [16].
- During the tests of activities directed to the midline, the subjects will be seated in a chair without an armrest (40 cm high) with the dorso-lumbar region of the spine supported on the back of the chair, next to a table (75 cm height), with the feet well supported on the floor, knees and hips flexed at 90º. The upper limbs are placed on the table, assuming as the initial position the shoulder in neutral position, elbow flexed at 90º, forearm in pronation, wrist in neutral position and two in extension.
- In activities directed to the contralateral side, participants are seated in a chair, in the same position as in the previous activities, but away from the table. The upper limbs are supported on the thighs, shoulders in a neutral position, elbows flexed at 45º, forearms and wrists in a neutral position and fingers semi-flexed. In these activities, only an object (hairbrush) is used, which is in the subject's hand in the initial position. To carry out these activities, a glass cup, a metal spoon, a soup bowl, a toothbrush, a toothpaste, and a hairbrush were selected as materials (Table I).
- The materials will be placed before the start of the rehearsal of each of the respective activities, in the respective marks on the table towards the midline of the subjects' body: the cup at the 8x8cm mark 30 cm from the edge of the table, the soup bowl at the 14x14 cm mark at 3 cm from the edge of the table and the toothbrush and toothpaste in the same mark.
- Before data collection, each activity is explained and given the opportunity to perform the movement so that subjects feel comfortable with the execution of it [10].
- Participants will be instructed to perform 5 trials in each of the 5 activities, making a total of 20 trials.
- Once the subjects are ready, the command "you can start now" is given and the subject will perform the activity at a speed comfortable for him/herself and five trials are collected.
- Between each trial, subjects will have a 2-minute rest period and a further rest period (5 minutes) between the set of activities aimed at the midline and activities aimed at the contralateral side to minimize muscle fatigue.

D. *Activities performed*

The activities performed by the participants consist of complex movements of the joints of the upper limbs. Considering their complexity, it is important to distinguish their phases [11][24] (Table I), as well as the respective movements performed by the shoulder [20] (Table II).

TABLE I. ACTIVITY PHASES IN ADLS

Activities Phases			
Activities to the midline		***Activities to the contralateral side***	
1.Starting position to reaching	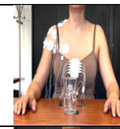	1.Grasping	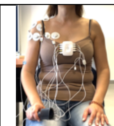
2.Grasping		2.Transporting to the contralateral side	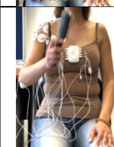
3.Transporting to the mouth	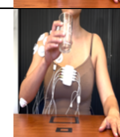	3.Reaching the contralateral side	
4.Introduced in the mouth	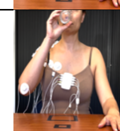	4.Return to the thigh	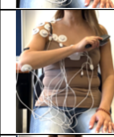
5.Return to the pick point	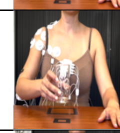	5.Return to initial position	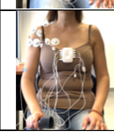
6.Return to initial position	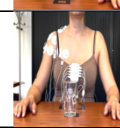		

TABLE II. EXPECTED MOVEMENTS BY PHASE.

Activity phases	**Activities to the midline**		
	Drinking	***Eating soup***	***Brushing teeth***
1.Starting position to reaching	AD, F	AD, F, SE	AD, F, SE
2. Grasping	AD, F, SE	AD, F, SE	AD, SE, F
2. Introduced to the mouth	F, ABD, SE	F, ABD SE	F, ABD, SE
4.Transporting to the mouth	F, ABD, SE	F, ABD SE	F, ABD, SE
5. Return to the pick point	AD, E, SE	AD, E, SE	AD, E, SE
6. Return to the initial position	E, SE, ABD	E, SE, ABD	E, SE, ABD
Activity phases	**Activities to the contralateral side**		
	Drinking	***Eating soup***	***Brushing teeth***
1.Grasping	AD	AD	AD
2. Transporting to the contralateral side	F, AD, SE	F, AD, SE	F, AD, SE
3.Reaching the contralateral side	F, AD, SE	F, AD, SE	F, AD, SE
4.Return to the thigh	E,ABD, SD	E, ABD, SD	E, ABD, SD
5.Return to initial position	E,ABD, SD	E, ABD, SD	E, ABD, SD

TABLE III. MEANS OF THE AMPLITUDE AND TIME OF PEAKS OF MAXIMUM AMPLITUDE.

	Activities to the midline					
	Drinking		***Eating soup***		***Brushing teeth***	
	Amplitude contraction peak (mV)	Time amplitude peak (s)	Amplitude contraction peak (mV)	Time amplitude peak (s)	Amplitude contraction peak (mV)	Time amplitude peak (s)
Pectoral Major	367 ±37	2.83 ±0,25	639 ±408	3.08 ±0,30	448 ±90	3.57 ±0,20
Anterior Deltoid	1970 ±218	2.42 ± 0,08	1665 ±239	2.73 ±0,23	1355 ±138	4.13 ±0,33
Middle Deltoid	1203, ±134	2.96 ±0,26	1144 ±132	2.30 ±0,26	757 ±63	5.05 ±0,46
Posterior Deltoid	413 ±39	3.43 ±0,28	402 ±42	2.24 ±0,22	341 ±34	4.01 ±0,55
Upper Trapezius	1893 ±265	2.56 ±0,24	2244 ±337	2.53 ±0,17	1976 ±238	4.42 ±0,41
Lower Trapezius	532 ±83	2.71 ±0,29	375 ±56	2.88 ±0,37	1445 ±1005	3.55 ±0,50

TABLE IV. MEANS OF THE AMPLITUDE AND TIME OF PEAKS OF MAXIMUM AMPLITUDE.

	Activities to the contralateral side			
	Arm washing		***Brushing the hair***	
	Amplitude contraction peak (mV)	Time amplitude peak (s)	Amplitude contraction peak (mV)	Time amplitude peak (s)
Pectoral Major	1190 ±181	1.72 ±0.10	855 ±135	1.71 ±0.10
Anterior Deltoid	2171 ±23	1.46 ±0.71	3134 ±360	1.52 ±0.80
Middle Deltoid	1112±117	2.20 ±2.67	1891 ±220	1.67 ±0.10
Posterior Deltoid	538 ±80	2.15 ±0.27	550 ±44	1.92 ±0.25
Upper Trapezius	1216 ±145	1.88 ±0.28	1952 ±269	1.57 ±0.16
Lower Trapezius	382 ±40	1.73 ±0.16	413 ±46	1.59 ±0.10

E. Signal Analysis

MATLAB software, version R2022a, was used to process the EMG signals. The files were imported into this software, and channels related to the EM activity were selected for each of the activity.

After selecting the epoch of 7000 points corresponding to the activity (part of the signal to be analyzed), the sample points were transformed into units of time (s), the mean of the signal was subtracted, the signal was placed in absolute values, and a moving mean was applied at the same.

Although most studies opt for a normalization of the contraction amplitude, we chose to obtain the values of the maximum peak amplitude (mV) of activation of each of the analyzed muscles and the time (s) in which they were in the activity, considering it as an advantage to be able to compare our results with the results of the previous study [16].

For the descriptive statistical treatment of data (mean and standard deviation) the Statistical Package for the Social Sciences (SPSS) software, version 28, was used.

III. RESULTS

The information on the maximum amplitude peaks (mV) of each muscle and the time (s) at which they occur during the performance of activities are presented in Table III (ADLs for the midline) and in Table IV (ADLs for the side contralateral). Graphs are also presented that exemplify, in a subject, the signal obtained in each of the ADLs performed, Figures 1, 2 and 3 (ADLs directed to the midline) and Figures 5 and 6 (ADLs directed to the contralateral side). It is verified in Table III that the ADLs directed to the midline (drinking from a glass, eating soup and brushing teeth) present a sequence of the average of the peaks of maximum amplitude of muscle activation that are different from each other, as well as the temporal sequence in which they occur also differs between them.

The only similarity verified is related to the muscles that present greater amplitude peaks, that is, the AD, UT, and MD (drinking from a glass and eating soup are common). The activity of brushing the teeth has in common with the two previous activities the UT and the AD (Table III).

Like with the previous activities, in Table IV, it is verified that ADLs directed to the contralateral side (washing the arm and brushing the hair) present a sequence of the average of the peaks of maximum amplitude of muscle activation that are also different from each other, as well as the temporal sequence in which they occur. The only similarity is the fact that the AD and UT are among the muscles that reach the highest amplitude peaks during the activity, as well as the PD and the LT among those that reach the lowest amplitude (Table IV).

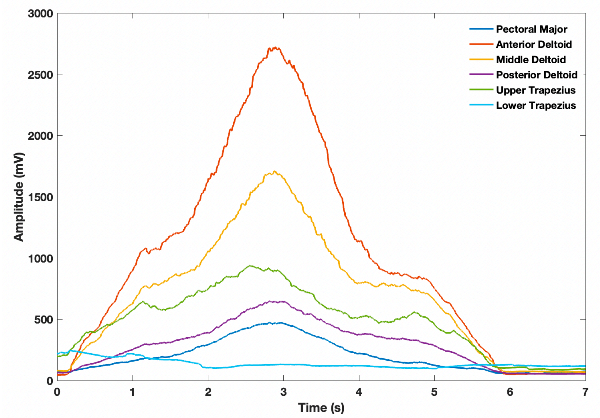

Figure 1. Amplitude pattern of muscle activation over time of drinking from a cup activity

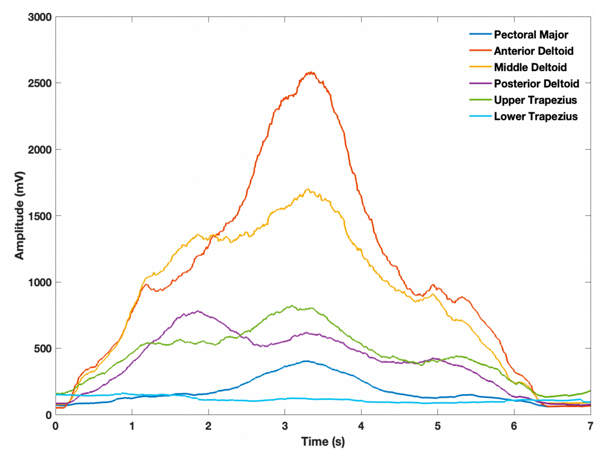

Figure 2. Amplitude pattern of muscle activation over time of eating soup activity.

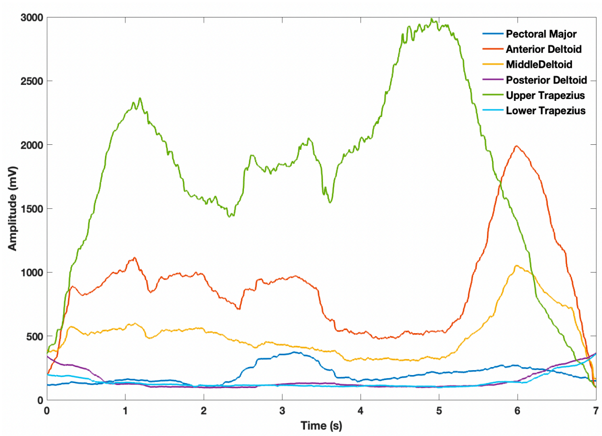

Figure 3. Amplitude pattern of muscle activation over time of brushing teeth activity.

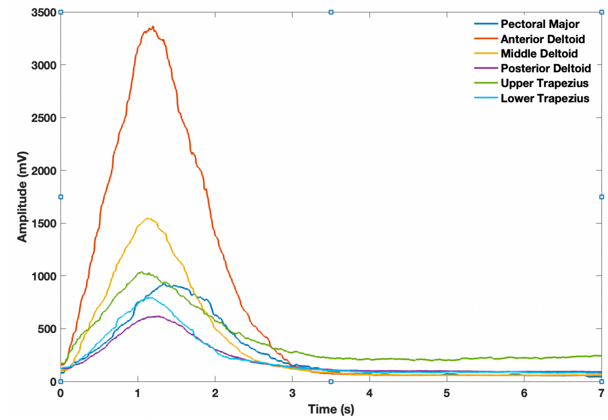

Figure 4. Amplitude pattern of muscle activation over time of washing the upper limb activity

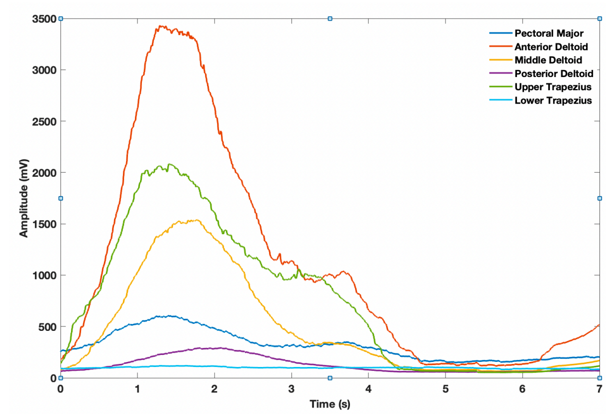

Figure 5. Amplitude pattern of muscle activation over time of brushing hair activity.

Regarding the period in which the average peaks of maximum muscle activation amplitude are found during the activity, we can see in Table III that the ADLs directed to the midline occur between 2.24s and 5.05s. In the activity of drinking from a glass, they occur in the interval of 1.01s (2.42s ± 0.08s and 3.43s ±0.28s), in eating the soup between 0.84s (2.24s ±0.22s and 3.08s ±0.30s) and brushing the teeth. between 1.5s (3.55s ±0.50s and 5.05s ±0.46s).

In the ADLs directed to the contralateral side, it is verified in Table IV, that the averages of the maximum amplitude peaks of muscular activation occur between 1.46s and 2.25s. In the activity of arm washing, they occur in the interval of 0.79s (1.46s ±0.71s and 2.20s ±2.67s), in brushing the hair between 0.4s (1.52s ±0.80s and 1.92s ±0.25s).

Regarding the pattern of muscle amplitude activation, five graphs representing the muscle activation pattern of one of the subjects, for each of the five ADLs, are presented. In these graphs, in all activities, there is a phase corresponding to the increase in muscle activation amplitude, in which after each muscle reaches it maximum amplitude (Tables III and IV), there is a decrease in it. This can be seen in Figure 1 (drinking), Figure 2 (eating soup) and Figure 3 (brushing teeth), corresponding to ADLs directed to the midline. Figure 4 (washing the arm) and Figure 5 (brushing the hair) concern ADLs directed to the contralateral side.

IV. Discussion and Critical Perspective

Regarding the analysis of the average times in which the maximum amplitude peaks occur, it is verified that in the ADLs directed to the midline, such as drinking or eating soup, the muscles reach an average of their maximum activation peaks at around 2 to 3 seconds. This reinforces the results of previous studies [16]. However, the same is not verified for the activity of brushing teeth, in which the time interval corresponding to the average in which the peaks of maximum amplitude occur is around 3 to 5 seconds (Table III).

In ADLs directed to the contralateral side, the average time in which the peaks of amplitude occur are between 1 and 2 seconds, which corroborates previous studies [16]. The results referring to the period in which the peaks occur are indicative that there are two marked phases in all activities. These phases are also represented in the graphs that constitute examples of the signal collected in each of the activities.

The first phase, in which there is an increase in the amplitude of muscle activation, corresponds to an increase in contraction. A second phase follows, in which there is a decreased amplitude, that is, decreased muscle contraction.

From ADLs directed to the midline and considering Table II, and other studies that mention these same phases of activity [11][16][24], it can be inferred that the contraction phase corresponds to the first four phases of activity, and the decreased contraction to the remaining phases.

Regarding the ADLs directed to the contralateral side (Figures 4 and 5) and the phases of these same activities (Table II), it can be inferred that the contraction phase corresponds to the first three phases of the activity, and the decreased contraction to the remaining phases.

In ADLs directed to the midline, the sequence of muscle amplitude activation peaks is different between the three activities (drinking, eating soup and brushing teeth) (Table III).

This difference may be related to the different requirements of the activities themselves, in each of the phases. In each of the ADLs directed to the midline, there are different procedures, which leads us to infer that in the same phase, despite the same muscles being involved, the amount of muscle fibers that are recruited for the performance of that phase in each of the activities is different. The same happens with ADLs directed to the contralateral side, in which both activities are different in the sequence of mean values related to the maximum peaks. The sequence of the average of the peaks of activation of the maximum muscle amplitude is different between the two activities (washing the contralateral arm and brushing the hair), as shown in Table IV.

To better understand this fact, it would be necessary to analyze the average values representative of the entire muscle activation amplitude during the activity and not just the average of the maximum activation peaks, or the graphs of only one subject in the sample.

V. Conclusion

Although the shoulder muscle groups involved in ADLs are the same, the specifics of the activity point to the existence of different characteristics in the amplitude of muscle activation between the ADLs analyzed. Thus, the results are indicative of differences in the pattern of peak muscle activation amplitudes, as well as in the time sequence in which they occur, between ADLs directed to the midline, between ADLs directed to the contralateral side, as well as between these two groups of activities.

There is a need for future work to understand these indications in a larger sample, with an average age closer to the average age of subjects with stroke and with data analysis that includes the normalization of the amplitude of muscle activation throughout the activities, relating it to a with the different phases of the activities. Another suggestion is the use of EMG in conjunction with other technologies, such as accelerometry and optoelectronic motion capture systems.

This study thus contributed to establish a normative behavior of shoulder movements during ADLs in a healthy population, which, in the future, can be compared with the results using the same experimental protocol in patients with pathologies such as stroke.

Acknowledgment

This work was supported by national funds from FCT – Foundation for Science and Technology, I.P. through the project UIDB/FIS/04559/2020 (LIBPhys-UNL).

References

[1] J. G. Broeks, G. J. Lankhorst, K. Rumping, and A. J. Prevo, “The long- term outcome of arm function after stroke: results of a follow- up study,” Disabil Rehabil, vol 21, pp. 357–364, Aug. 1999, doi:10.1080/096382899297459.

[2] H. Nakayama, H. S. Jorgensen, H. O. Raaschou, and T. S. Olsen, “Recovery of upper extremity function in stroke patients: the Copenhagen Stroke Study,” Arch Phys Med Rehabil, vol 75, no. 4, pp. 394–398. Apr.1994, doi:10.1016/0003-9993(94)90161-9.

[3] V. M. Parker, D. T. Wade, and R. Langton Hewer, “Loss of arm function after stroke: measurement, frequency, and recovery,” Int Rehabil Med, vol. 8, no. 2, pp. 69–73, 1986, doi:10.3109/03790798609166178.

[4] J. A. Beebe and C. E. Lang, “Absence of a proximal to distal gradient of motor deficits in the upper extremity early after stroke,” Clin Neurophysiol, vol. 119, no. 9, pp. 2074–2085, Sep. 2008, doi:10.1016/j.clinph.2008.04.293

[5] K. J. Wisneski and M. J. Johnson, “Quantifying kinematics of purposeful movements to real, imagined, or absent functional objects: implications for modelling trajectories for robot-assisted ADL tasks,” J Neuroeng Rehabil, vol. 4, no. 7, pp. 1–14, Mar 2007, doi:10.1186/1743-0003-4-7.

[6] A. L. Foundas *et al.,* “Ecological implications of limb apraxia: evidence from mealtime behavior,” J Int Neuropsychol Soc, vol. 1, no. 1, pp. 62–66, Mar 2007, doi:10.1017/s1355617700000114.

[7] M. M. Bieńkiewicz, M. L. Brandi, G. Goldenberg, C. M. Hughes, and J. Hermsdörfer, " The tool in the brain: apraxia in ADL. Behavioral and neurological correlates of apraxia in daily living," Front Psychol, vol. 5, no. 365, pp. 1–13, Apr 2014, doi:10.3389/fpsyg.2014.00353

[8] G. W. Humphreys and E. M. E. Forde, "Disordered action schema and action disorganisation syndrome," Cogn. Neuropsychol, vol. 5, pp. 771–811, Sep. 2018.

[9] P. H. McCrea, J. J. Eng, and A. J. Hodgson, "Biomechanics of reaching: clinical implications for individuals with acquired brain injury," Disabil Rehabil, vol. 24, no. 10, pp. 534–541, Jul. 2002, doi:10.1080/09638280110115393.

[10] M. Alt Murphy, C. Willén, and K. S. Sunnerhagen, "Kinematic variables quantifying upper-extremity performance after stroke during reaching and drinking from a glass," Neurorehabil Neural Repair, vol. 25, no. 1, pp. 71–80, Jan. 2011, doi:10.1177/1545968310370748.

[11] K. Kim *et al.*, "Kinematic analysis of upper extremity movement during drinking in hemiplegic subject," Clin Biomech, vol. 29, no. 3, pp. 248–256, Mar. 2014, doi:10.1016/j.clinbiomech.2013.12.013.

[12] G. L. Santos and T. L. Russo, A. Nieuwenhuys, D. Monari, K. Desloovere, "Kinematic Analysis of a Drinking Task in Chronic Hemiparetic Patients Using Features Analysis and Statistical Parametric Mapping," Arch Phys Med Rehabil, vol. 99, no. 3, pp. 501–511, Mar. 2018, doi:10.1016/j.apmr.2017.08.479.

[13] F. Molina Rueda *et al*., "Movement analysis of upper extremity hemiparesis in patients with cerebrovascular disease: a pilot study," Neurologia, vol. 27, no. 6, pp .343–347, Jul. 2012, doi:10.1016/j.nrl.2011.12.012

[14] F. B. van Meulen, J. Reenalda, J. H. Buurke, and P. H. Veltink, "Assessment of daily-life reaching performance after stroke," Ann Biomed Eng, vol. 43, no. 2, pp .478–486, Feb. 2015, doi:10.1007/s10439-014-1198-y.

[15] G. Thrane, K. S. Sunnerhagen, and M. A. Murphy, "Upper limb kinematics during the first year after stroke: the stroke arm longitudinal study at the University of Gothenburg (SALGOT)," J Neuroeng Rehabil, vol. 14, no. 1, pp .1–12, Jun. 2020, doi:10.1186/s12984-020-00705-2.

[16] P. Santos, C. Quaresma, I. Garcia, and C. Quintão, "Neuromotor Evaluation of the Upper Limb During Activities of Daily Living: A Pilot Study" Technological Innovation for Digitalization and Virtualization (DoCEIS 2022), IFIP Advances in Information and Communication Technology, vol. 649, pp. 112–121, Jun. 2022, doi: 10.1007/978-3-031-07520-9_11.

[17] N. Abas, W. M. Bukhari, M. A. Abas, and M. O. Tokhi, "Electromyography assessment of forearm muscles: Towards the control of exoskeleton hand" in 5th International Conference on Control, Decision and Information Technologies (Codit 2018), Instituto of Eletrical and Eletronics Engineers, pp. 2-6, Apr. 2018, doi: 10.1109/CoDIT.2018.8394906.

[18] L. Dipietro *et al*., "Changing motor synergies in chronic stroke," J Neurophysiol, vol. 98, no. 2, pp. 757–768, Aug.. 2007, doi:10.1152/jn.01295.2006.

[19] C. J. van Andel, N. Wolterbeek, C. A. Doorenbosch, D. H. Veege, and J. Harlaar, "Complete 3D kinematics of upper extremity functional tasks," Gait Posture, vol. 27, no. 1, pp. 120–127, Jan. 2008, doi:10.1016/j.gaitpost.2007.03.002

[20] J. Esperança Pina. Locomotion Anatomy, 4th ed.. Lisbon: Lidel, 2017.

[21] A. M. Oosterwijk, M. K. Nieuwenhuis, C. P. van der Schans, and L. J. Mouton, "Shoulder and elbow range of motion for the performance of activities of daily living: A systematic review," Physiother Theory Pract, vol. 34, no. 7, pp .505–528, Feb. 2018, doi:10.1080/09593985.2017.1422206

[22] Plux, Wireless Biosignals, "Biosignals plux:user manual", Pliux, Lisbon. Consultado em Jun. 06,2022.[online]. Available:https://support.pluxbiosignals.com/wp-content/uploads/2021/11/biosignalsplux_User_Manual.pdf.

[23] H. J. Hermens, B. Freriks, C. Disselhorst-Klug, and G. Rau, "Development of recommendations for SEMG sensors and sensor placement procedures," J Electromyogr Kinesiol, vol. 10, no. 5 pp .361–374, Oct. 2000, doi:10.1016/s1050-6411(00)00027-4.

[24] M. Alt Murphy, S. Murphy, H. Persson, U. Bergström, and K. Sunnerhagen, "Kinematic Analysis Using 3D Motion Capture of Drinking Task in People With and Without Upper-extremity Impairments," J Vis Exp, vol. 28, no. 133, pp.1–9, Mar. 2018, doi:10.3791/57228.

Electrophysiological Answer to a Checkerboard Stimulus: A Pilot Study

Ana Isabel Ferreira
Physics Department, LIBPhys, NOVA School of Science and Technology; 2829-516 Caparica, PT
Health Department, Higher School of Health, Polytechnic Institute of Beja, 7800-111 Beja, Portugal
aix.ferreira@campus.fct.unl.pt

Ana Ferrão
Physics Department, NOVA School of Science and Technology, Almada, Portugal
acp.ferrao@campus.fct.unl.pt

Catarina Andrade
Physics Department, NOVA School of Science and Technology, Almada, Portugal
cs.andrade@campus.fct.unl.pt

Mónica Baptista
Central Lisbon University Hospital Center; Lisbon, Portugal
monica.baptista@chlc.min-saude.pt

Cláudia Quaresma
Physics Department, LIBPhys, NOVA School of Science and Technology, Almada, Portugal
q.claudia@fct.unl.pt

Carla Quintão
Physics Department, LIBPhys, NOVA School of Science and Technology, Almada, Portugal
cmquintao@fct.unl.pt

***Abstract*—Electroencephalography is a clinical signal that reveals the brain's electrical activity. In this category, the Visual Evoked Potentials (VEP) is one of the most frequent measures, especially when it is necessary to assess the maturity and function of the central visual system. The Electrodermal Activity (EDA) data gives information about skin conductance, and it is used to evaluate autonomic sympathetic reactions, often related to neuropsychological states. It could be used with all ages and in young subjects with healthy development or clinical practice with children with atypical development. In this paper, we propose an experimental setup based on checkerboard stimuli to assess the evolution of visual system development of preterm infants. This experimental protocol was applied to two female preterm born infants of 4 and 6 months of corrected age. The preliminary findings show that, as expected, the P100 latencies and amplitude are still different from those expected for adults and older children. However, the older infant presents results more similar to adults, corresponding to having a more mature visual system. Concerning EDA, it was observed that the older infant presents more responses to the stimulus, a higher level of skin conductance, and a shorter latency time than the younger infant, which is congruent with what is expected, given the maturation of the nervous system. The methodology used in this pilot application and the algorithm defined seem adequate to use in a longitudinal study to follow the evolution of preterm and term infants.**

Keywords - Electrophysiology; visual evoked potentials; electrodermal activity; preterm born.

I. INTRODUCTION

Electroencephalography is used in neuroscience to explore the electrical activity of living neurons. These cells communicate using electrical and chemical signals, and electroencephalographic techniques aim to measure this activity non-invasively [1]. The electroencephalography signals have been measured since the XIX century [2], but optimization of signal processing techniques has helped uncover information that changed the way various diseases were diagnosed previously [3].

Visual Evoked Potentials (VEP) are massed electrical signals generated by occipital cortical areas in response to visual stimulation [4]. Specifically, the VEPs are utilized in research and clinical practice to characterize the function and integrity of the visual system, mainly optic nerve lesions, optic neuritis, and multiple sclerosis [5]. Those bioelectric signals generated in the striate and extrastriate cortex by retinal stimulation could be recorded from the scalp using electrodes [5] positioned in the specific Brodman Area 17, 18, and 19 [4] that can provide important diagnostic information regarding the functional integrity of the visual system [6].

Different stimuli are currently used to analyze the visual cortex response. These could be divided into two kinds of visual stimuli: unpatterned flashing lights and patterned stimuli. The most used pattern is a checkerboard with black and white squares [5]. In a pattern-reversal paradigm, the pattern is alternated without change in the luminance at a specific reversal rate [4]. Although the most used sample rate is 2 reversals per second [6], other taxa could be used with specific populations [7]-[10]. With that kind of stimuli, the typical waveform consists of N75, P100, and N135 peaks [6].

In traditional methodologies, the assessment is done in a specific location using fixed equipment. However, current clinical and research demands lead to developing portable devices, like g.Nautilus© [11] allows for a dependable data

 ISBN: 978-1-68558-004-9

recorder at the subjects' location. To assess is necessary to be stationed in a quiet room, guaranteed a typical ambient light level, correct positioning of the electrodes, and participants at least 70 cm from the stimulus [12]. To record the data, single electrodes could be used in occipital positions or a CAP where the electrodes are already positioned. This system's advantage is that the sensors' correct positioning is guaranteed. However, regardless of the system to position the sensors, they must be connected with the software that registers the signal and connects to the visual stimuli.

The Electrodermal Activity (EDA) signal is an electrical manifestation of the sympathetic innervation of the sweat glands. EDA has had a history in psychophysiological research (including emotional or cognitive stress) since the middle of XIX century. It is measured in a non-invasive skin surface mode, predominantly from plantar eccrine sweat glands [13].

In recent years, researchers began using EDA for pathophysiological applications like assessing fatigue, pain, sleepiness, exercise recovery, diagnosis of epilepsy, neuropathies, and depression, among others [14]. A recent study with newborns has shown that EDA parameters seem sensitive in detecting sympathetic regulation changes in early postnatal life. The EDA measure can represent an essential step towards a non-invasive early diagnosis of the pathological states linked to autonomic dysmaturation in newborns [15]. Although the skin biomarkers of preterm birth could be seriously altered [16], the EDA of that population has not been measured, associated with a visual stimulus, as far as we know.

Preterm born is a condition that has increased in the last few decades, and it is estimated by World Health Organization that 15 million infants are born too early every year. That represents more than 1 in 10 infants [17]. The consequences of preterm birth have a large spectrum of variability. Some infants without any permanent sequelae at 2 years old have the same motor development as full-term infants at the same age [18]. However, unfortunately, most infants suffer the consequences of being preterm born for a longer period [17] in ways that could be subtle or more apparent, with impacts on growing, playing, or learning [19]-[21]. Despite the knowledge about the changes in different areas of participation, the link between those and electrophysiological signals patterns and the early biomarker identification is not completely established. Accepting the electroencephalography response as a quantitative signal of nervous system function and knowing its selective use in clinical settings, our research group is motivated to deeper understand the VEP and EDA in the first months of life of preterm born infants. In order to answer the previously identified requirements for visual skills assessments [22] and enlarge the clinical and developmental follow-up evaluations that already exist, this paper aims to present an integrated experimental setup to assess the evolution of visual system development in preterm infants. It also presents the results of a pilot application with two preterm infants.

To achieve these goals, the proceeding was organized to describe the materials and methods used, followed by results presentation and analysis, finishing with the conclusions and suggestions for further work.

II. MATERIALS AND METHODS

This section describes the experimental setup as well as the main procedures of data collection and analyses used.

The study was authorized by the Ethical Commission of Central Lisbon University Hospital Center with the official reference "Projeto INV14", and the parents gave written informed consent.

A. Experimental setup

As seen in Fig. 1, the experimental setup integrates the following equipment:

- Computer: all the equipment runs on a Dell Computer (Intel ® Core (TN) 2DUO, 4,00 GB) that projects the image for a LG flatron W1934s;
- E-Prime®: software used to create the visual stimuli, black/white checkerboard pattern;
- g.Nautilus®: serial number NB-2017.08.77 was used with software g.Recorder® version 5.16.00 and allows recording of the VEP. The connection between the g.Nautilus© and E-Prime was done using a parallel port;
- Biosignalsplux®: used with the opensignals® software to record EDA signals. The connection between biosignals and E-Prime was guaranteed by a socket that records the triggers related to the stimuli appearance.

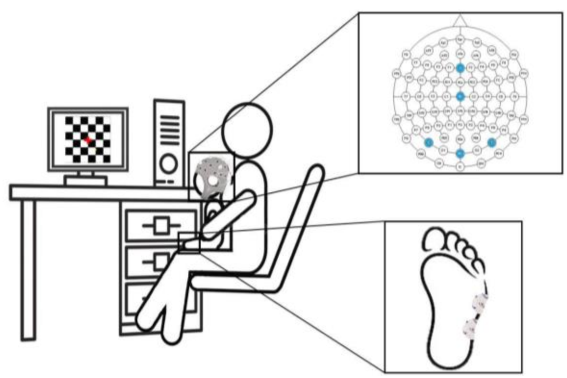

Figure 1: Experimental setup

As previously referenced, the visual stimuli were created using the E-Prime® software. A pattern-reversal evoked potentials technique was chosen, creating a checkerboard pattern in which the colors of the squares (black and white) were inverted every 1 second for a total of 120 seconds. The choice of this pattern was based on the fact that it presents a lower variability in latency and amplitude between different measurements, which facilitates data comparison [4]. Furthermore, the number of stimuli presented was thought to be comprehensive enough to allow several parts of the signal to be still used, considering that it would be almost impossible not to have many artifacts in the infants' signals. At the center of the checkerboard pattern, there is a red cross that serves as a fixation point to look at. Before and after the pattern is shown, warning messages about the start and end of signal acquisition are displayed to the participants. It is also important to note that the chosen inversion timing was inspired by previous studies implemented with preterm born infants [7][8]. Since the correct creation of VEP depends on the exact moment that the presentation of each stimulus is precisely marked, the connection between E-Prime® and the software that allows data collection (g.Nautilus®) was made. To accomplish this, E-Prime® has been parameterized to send a signal each time the checkerboard pattern was reversed (trigger moment). The parameterization was based on the instructions in the g.Recorder© - Parallel Port QuickStart script V5.16.00 referring to g.Nautilus® software. As for the acquisition rate, it was defined that it would use 250 Hz due to the equipment specifications.

B. Data collection procedures

The electrophysiological measurements were done with the infant on the parent's lap and using the infant's binocularity. Related to the VEP, the data collection was done using the g.Nautilus® software, whose equipment consists of a cap with 32 active channels. In the present study, the international 10/20 electrode placement system [6] was used, and the electrodes corresponding to PO7, PO8, Oz, Cz, Fz, and ear lobe, as reference electrode, are recorded. After placing the correct size cap, Sigma Gel was distributed over the electrodes to reduce the impedance, measured with the g.NEEDaccess® - Demo Client software. Considering that active electrodes were used, it was defined that the collection of the signals was ready to be done when the impedance of all the electrodes was less than 30 kΩ.

Regarding the EDA, the data collection was performed with Biosignalsplux®. To measure the electrodermal signal, an EDA sensor, including two channels was used, with two electrodes attached to it. The acquisition rate was defined at 500Hz, in order to collect as much information as possible. This methodological option was taken since this is an exploratory study.

On the computer, Opensignals®, a software that allows the observation of the data collected with Biosignalsplux® in real time, was required. The data was acquired via Bluetooth communication and archived in ".txt" and ".h5" formats. Identical to the collection for VEP, for the study of EDA, the aforementioned visual stimulus created with E-Prime© was used.

Since the correct processing of the signal depends on marking the exact moment of the presentation of each stimulus, a connection was made between E-Prime and Opensignals in addition to the link between E-Prime and g.Nautilus already mentioned. For EDA, the connection between the two software programs was achieved using a socket, as suggested in the E-Prime Guide [23], and triggers were placed at the beginning and end of the stimulus presentation. For the further processing of the signal, this placement was taken into account and, with the use of the file saved by g.Nautilus®, it was possible to access the remaining triggers (obtained each time the checkerboard pattern was reversed). This parametrization was chosen since having the exact trigger moment for both connections (E-Prime®-Opensignals® and E-Prime®-g.Nautilus®) showed some incompatibilities.

C. Processing signals methodologies

For both VEP and EDA, signal processing was performed with MatLab® software.

For VEP, the signal processing started with removing the direct current component by subtracting its own average from each signal. Then, to improve the signal quality, it was decided to apply a filter prior to the average of the signal epochs corresponding to each stimulus. Based on previous studies using Butterworth filters [24] and filters with cut-off frequencies between 2.5 Hz [25] and 30 Hz, [26] the choice fell on:

- used the Filter Designer tool provided by MatLab® to design the filter;
- applied for a 4th order Butterworth bandpass filter with cut-off frequencies of 2 Hz and 30 Hz;
- applied the *filtfilt* function to prevent signal delay after the filter application.

Finally, the signal was divided into 120 epochs, each corresponding to a reversal of the checkerboard pattern. Therefore, for the entire evoked response to be visible, the cuts performed on the signal must be done a few milliseconds before and after the exact moment of the stimulus. In this way, the moments immediately prior to the application of the stimulus (baseline) are observed, as well as the total response to the stimulus that is prolonged in time. Thus, it was decided to cut the signal 100ms before and 700ms after viewing the pattern reversal. Consequently, these epochs were averaged by adding them and dividing them by the number of epochs.

As the result continued to present a lot of noise, the application of a low-pass filter was studied [27] and created again with the Filter Designer application and with the specification:

- applied with the *filtfilt* function;
- a 4th order low-pass Butterworth filter with a cut-off frequency of 10 Hz.

To make visualization of VEP formation more intuitive, an interface was created with the GUIDE tool provided by

MatLab®. From left to right, the first graphics on the interface show the signal obtained considering only the first 20 seconds, then considering 40 seconds and continuing to increase the time window until the final result. The remaining graphs show the evoked responses corresponding only to specific 20-epoch plots of the signal. The method described above was tested in adults, and the results showed that the algorithm developed effectively processed the VEP. However, for some children, it was found that the signal was still contaminated with artifacts. Knowing that the standard deviation can be used for artifact's detection [28] and testing threshold values, the method chosen was to eliminate the segments whose standard deviation was 0.6 times higher than the standard deviation of the signal segment, being this value heuristically found.

Since the EDA signal is composed of two different components, phasic and tonic [29], it was helpful to analyze them separately. This was performed using Ledalab©, a Matlab© toolbox that allows the decomposition of the signal and extraction of some parameters from the phasic component, which has information related to response to the stimulus. The signal processing began by reading the .txt file extracted from Opensignals® and the .hdf5 file from g.Nautilus®. The next step consisted of converting the raw data and downsampling the result data from 500 Hz to 100Hz to facilitate its analysis in Ledalab®. Next, a moving average filter, with a window of 50 sample points, was also applied to smooth the signal without losing relevant information. After this, Ledalab® was executed with two files: a file containing the converted values of EDA as input and the file with the trigger moments information, created with the g.Nautilus® software. The separation of the two components, phasic and tonic, was performed using the Discrete Decomposition Analysis [30], as it allows the individual study of each electrodermal response and presents a detailed time discretization. From this step, a graph like the one represented in Fig. 2 is obtained.

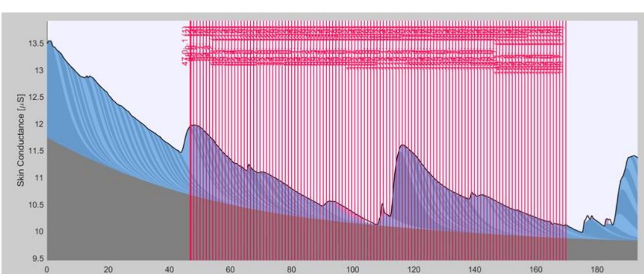

Figure 2: Result from non-negative deconvolution. It is possible to observe the separation between the tonic EDA, in grey, and the phasic EDA, in blue. The red lines represent the recorded trigger moments.

Afterward, parameters such as the number of responses, latency time, amplitude, area, and conductance level were extracted, only the responses in a time window of 0.5s to 1s from each stimulus (to extract specific responses to the stimuli before the next one occurs as mentioned previously the reversal rate is 1s) and with amplitude above 0.01 μS [31].

D. Sample characterization

The present pilot application was conducted with two preterm born infants (P.1 and P.2), followed by an outpatient development appointment of Dr. Alfredo da Costa Maternity. The two female infants in the pilot study did not have major lesions (periventricular haemorrhage grade III or plus and /or retinopathy of prematurity grade III or more in cranial ultrasound done at age equivalent at term). Participant n. 1 was 30 weeks and 6 days of gestational age, 1945g birth weight and 4 months corrected age at data collection time. Participate n. 2 was 24 weeks and 5 days of gestational age, 685g birth weight and 6 months corrected age at data collection time.

III. Results Presentation and Analyses

In Fig 3, one can see an example of the electroencephalographic data recorded before, during and some time after the presentation of the stimuli. The epochs marked by a green bar were used to calculate the average and obtain the evoked potentials waveforms. The epochs marked by a red bar were removed since they were contaminated with artifacts. Given the results, we can conclude that, in both infants, most artifacts were found at the beginning and the end of the measurement, which could match the periods when they are still focusing on the stimulus and when they are tired of looking at it.

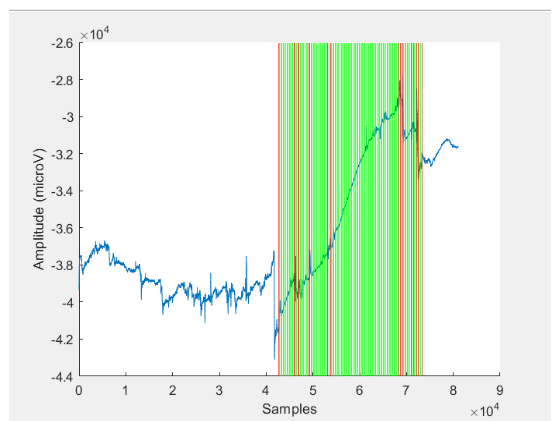

Figure 3: Selection of the signal epochs to use for processing (green epochs were included in the processing, and red epochs were excluded as artifacts)

The overview of the VEP results is presented in Fig. 4. Considering that P100 is one of the typical waveforms resulting from visual stimuli [6] in Table I, one can find the specific amplitude and latency of P100 obtained in PO8 electrode. In the following graphs, samples were converted to time for better understanding. As expected, latencies for the older child are lower, as her visual system is more mature [32]. It is also worth noting that the shape of the potentials for the two infants is "larger" than would be predicted for an adult, which is in agreement with the consulted literature [4] [7].

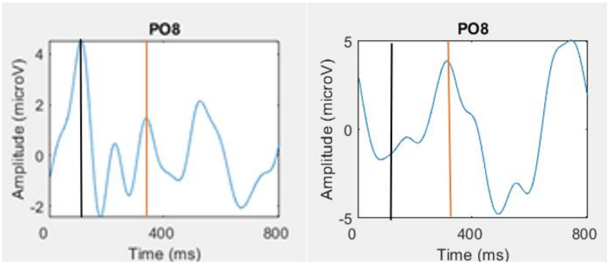

Figure 4: VEP of four (left) and a six-month (right) old infants with vertical lines to mark the stimulus presentation (black) and the P100 latency (orange)

TABLE I – LATENCY (MS) PER PARTICIPANT AND REGION

	PO8	CZ	PO7	Oz	Mean
P.1 (4M)	240	236	240	248	241
P.2 (6M)	212	192	232	212	212

Figure 5 shows the VEP change (blue line) during sample collection for the 6-month-old infant using the GUIDE interface. It was found that beyond 80 stimuli presented the result did not vary appreciably. As for the various plots of 20 epochs, there were some differences in their shape, probably due to changes in the state of attention.

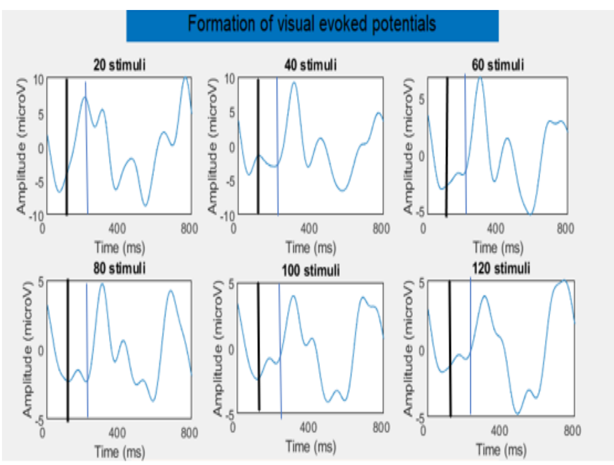

Figure 5: VEP changes during sample collection using GUIDE interface for a 6-month-old infant with vertical lines to mark the stimulus presentation (black) and the ideal P100 latency (blue). Each graph corresponds to adding 20 epochs to the signal processing from left to right.

The arousal state is one of the behavioral characteristics that could influence good-quality pattern VEP recordings [4]; this is why the present data were collected when infants were cooperative and calm. In that way is expected that negative components preceding and following the positivity appear at 2-4 months of age, and the waveform is adult-like by 68 months of age [10].

The methods previously described for the EDA were applied to the same preterm female infants for VEP. The parameters extracted from Ledalab© for both infants can be seen in Table II. However, due to the lack of reference values for these parameters in infants using visual stimuli in the current literature, it is not feasible to draw compelling conclusions with just this pilot application.

TABLE II – PARAMETERS EXTRACTED FROM LEDALAB FOR BOTH PARTICIPANTS

	Number of responses	*Amplitude (μS)*	*Area (nS^2)*	*Latency Time (s)*	*Skin conductance level (μS)*
P.1 (4M)	29	8.68	48.87	0.79	6.39
P.2 (6M)	38	4.51	37.11	0.75	10.15

Still, these two pilot applications already show some evidence conforming to what was expected according to the results obtained for other types of stimulation. Namely, the older infant presents a higher number of responses to the stimuli, a lower amplitude [33], a lower latency time [34], and a higher skin conductance level [35] in comparison to the younger one. These are all related to the maturation of the nervous system and, consequently, greater reactivity to the stimuli.

Those preliminary results align with a previous study that proposes pattern VEP as a valuable technique for monitoring visual development in preterm infants using corrected age [7]. The continuity of the study allows the build of a database with healthy preterm born visual development that could be compared with typical development. The early data from VEP and EDA could probably function as a physiological marker to detect some fragility when development is not following a typical stream.

IV. CONCLUSION AND FUTURE WORK

The pilot application showed that this experimental setup could be used to study VEP and EDA in infants, helping compare recordings from different age groups.

The experiment and algorithm developed by the research group allow the processing of data collected with very young infants with low cooperation capacity. The results proved that one could find significant differences in premature infants with an age difference of 2 months. Moreover, this experiment has shown that visual stimuli affect visual and electrodermal responses that can be corresponded to the infants' age. Thus, the combined analysis may correlate more effectively with infant development. Although the reduced sample size may be a limitation, the results show that the procedures implemented apply to young participants. Furthermore, the algorithm developed allows for noise remotion and reliable data analysis.

After this experimental protocol and setup testing, the research team is prepared to integrate the data collected with this electrophysiological setup with other clinical and developmental data. This way, it is possible to do a holistic assessment with longitudinal collections of signals in premature and full-term infants to compare the two groups and their evolution over time. In addition, this procedure allows the integration of data from statistically significant sample sizes in biomedical health records in children's healthcare systems.

ACKNOWLEDGMENT

The research group, mainly AIF, acknowledges the clinical team of Dr. Alfredo da Costa Maternity for the reception of the project idea and support across its implementation during infants' recruitment and assessment. Furthermore, national funds supported this work from FCT – Foundation for Science and Technology, I.P. through the project UIDB/FIS/04559/2020 (LIBPhys-UNL).

REFERENCES

[1] M. Carter and J. Shieh, "Chapter 4 – Electrophysiology", in Guide to Research Techniques in Neuroscience, 2nd ed., Academic Press, pp. 89-115, 2015, doi: 10.1016/B978-0-12-800511-8.00004-6

[2] E. Nierdermeyer and F. L. Silva., Electroencephalography basic principles, clinical applications and related fields, 3rd ed.,; Williams & Wilkins, 1993

[3] L. Sornmo and P. Laguna, Bioelectrical signal processing in cardiac and neurological applications, Academic Press, 2005, doi: 10.1016/B978-0-12-437552-9.X5000-4

[4] E. Birch and V. Subramanian, "Chapter 23 - Visual evoked potentials in infants and children", in Aminoff's Electrodiagnosis in clinical neurology, 6th ed., Elsevier, pp. 505-518, 2012

[5] R. Kothari, P. Bokariya, S. Singh and R. Singh, "A Comprehensive review on methodologies employed for visual evoked potentials", Scientifica (Cairo), 2016:9852194, Feb 2016, doi: 10.1155/2016/9852194

[6] J. Odom et al., " ISCEV standard for clinical visual evoked potentials: (2016 update)", Doc Ophthalmol., vol. 133(1), pp. 1-9, Aug 2016, doi: 10.1007/s10633-016-9553-y

[7] M. Roy, M. Barsoum-Homsy, J. Orquin and J. Benoit, "Maturation of Binocular Pattern Visual Evoked Potentials in Normal Full-Term and Preterm Infants from 1 to 6 Months of Age", Pediatric Research, vol. 37(2), pp. 140-144, Feb 1995, doi: 10.1203/00006450-199502000-00002

[8] E. Schwindt et al., "The impact of extrauterine life on visual maturation in extremely preterm born infants", Pediatric Research, vol. 84, pp. 403-410, Jun 2018, doi: 10.1038/s41390-018-0084-y

[9] B. Abrams and H. Waldman, "Chapter 14 - Electromyography and Evoked Potentials", in Practical Management of Pain, 5th ed., Mosby, pp. 162-184, 2014, doi: 10.1016/B978-0-323-08340-9.00014-1

[10] M. Taylor and D. McCulloch, "Visual Evoked Potentials in Infants and Children", Journal of Clinical Neurophysiology", vol. 9(3), pp. 357-372, Aug 1992, doi: 10.1097/00004691-199207010-00004

[11] G.Tec©, *g.Nautilus Research*, g.Tec©.[Online]. Available from: g.NAUTILUS RESEARCH | Wearable EEG Headset | g.tec medical engineering GmbH (gtec.at)

[12] American Clinical Neurophysiology Society, "Guideline 9B: Guidelines on visual evoked potentials", Journal of clinical neurophysiology: official publication of the American Electroencephalographic Society, vol. 23(2), pp. 138-156, Apr 2006, doi: 10.1097/00004691-200604000-00011

[13] J. Ham and E. Tronick, "A procedure for the measurement of infant skin conductance and its initial validation using clap induced startle", Dev Psychobiol., vol. 50(6), pp. 626-631, Sep 2008, doi: 10.1002/dev.20317

[14] H. Posada-Quintero and K. Chon, "Innovations in Electrodermal Activity Data Collection and Signal Processing: A Systematic Review", Sensors, vol. 20(2), pp. 479, Jan 2020, doi: 10.3390/s20020479

[15] Z. Visnovcova, M. Kozar, Z. Kuderava, M. Zibolen, N. Ferencova and I. Tonhajzerova, "Entropy Analysis of Neonatal Electrodermal Activity during the First Three Days after Birth", Entropy, vol. 24(3), pp. 422, Mar 2022, doi: 10.3390/e24030422

[16] M. Visscher et al., "Biomarkers of neonatal skin barrier adaptation reveal substantial differences compared to adult skin", Pediatric Research, vol. 89, pp. 1208-1215, Jun 2020, doi: 10.1038/s41390-020-1035-y

[17] World Health Organization, *Born too soon: the global action report on preterm birth*, World Health Organization., 2012. [Online]. Available from: https://apps.who.int/iris/handle/10665/44864

[18] M. Bracewell and N. Marlow, "Patterns of motor disability in very preterm children", Mental retardation and developmental disabilities research reviews, vol. 8(4), pp. 241-248, 2002, doi: 10.1002/mrdd.10049

[19] R. Silveira and R. Procianoy, "Preterm newborn's postnatal growth patterns: how to evaluate them", Jornal de Pediatria, vol. 95, supplement 1, pp. 42-48, Mar 2019, doi: 10.1016/j.jped.2018.10.006

[20] F. Finlayson, J. Olsen, S. Dusingd, A. Guzzetta, A. Eeles and A. Spittle, "Supporting Play, Exploration, and Early Development Intervention (SPEEDI) for preterm infants: A feasibility randomised controlled trial in an Australian context", Early Hum. Dev., 151:105172, Dec 2020, doi: 10.1016/j.earlhumdev.2020.105172

[21] A. Carmo et al., "Neurological, cognitive and learning evaluation of students who were born preterm", Rev. Paul. Pediatr, 40:e2020252, 2022, doi: 10.1590/1984-0462/2022/40/2020252

[22] A. Ferreira, C. Quintão and C. Quaresma, "Assessment of Visuomotor and Visual Perception Skills in Children: A New Proposal Based on a Systematic Review", Camarinha-Matos, L.M., Ferreira, P., Brito, G. (eds) Technological Innovation for Applied AI Systems. DoCEIS 2021, IFIP Advances in Information and Communication Technology, Springer, 2021, vol. 626, doi: 10.1007/978-3-030-78288-7_26

[23] PLUX – Wireless Biosignals, *E-Prime® integration in OpenSignals- Quick Start Guide*, PLUX – Wireless Biosignals. [Online]. Available from: OpenSignals E-Prime Integration - Quick Start Guide.pdf (plux.info)

[24] S. Dimitriadis and A. Marimpis, *Enhancing Performance and Bit Rates in a Brain–Computer Interface System With Phase-to-Amplitude Cross-Frequency Coupling: Evidences From Traditional c-VEP, Fast c-VEP, and SSVEP Designs*, Front. Neuroinform, vol.12, Mai 2018, doi: 10.3389/fninf.2018.00019

[25] M. Michalczuk, B. Urban, B. Chrzanowska-Grenda, M. Oziębło-Kupczyk and Alina Bakunowicz-Łazarczyk, *An Influence of Birth Weight, Gestational Age, and Apgar Score on Pattern Visual Evoked Potentials in Children with History of Prematurity*, Neural plasticity 2015, pp. 754864, Aug 2015, doi: 10.1155/2015/754864

[26] D. Birtles, O. Braddick, J. Wattam-Bell, A. Wilkinson and J. Atkinson, *Orientation and motion-specific visual cortex responses in infants born preterm*, NeuroReport, vol.18(18), pp. 1975-1979, Dec 2007, doi: 10.1097/WNR.0b013e3282f228c8

[27] M. O'Reilly et al., *Ophthalmological, cognitive, electrophysiological and MRI assessment of visual processing in preterm children without major neuromotor impairment*, Developmental Science, vol. 13(5), pp. 692-705, Aug 2010, doi: 10.1111/j.1467-7687.2009.00925.x

[28] I. Iturrate, R. Chavarriaga and J. del R.Millán, “Chapter 23 - General principles of machine learning for brain-computer interfacing” in Handbook of Clinical Neurology, Science Direct, pp. 311-328, 2020, doi: 10.1016/B978-0-444-63934-9.00023-8

[29] J. Braithwaite, D. Watson, R. Jones and M. Rowe, *A Guide for Analysing Electrodermal Activity (EDA) & Skin Conductance Responses (SCRs) for Psychological Experiments*, BIOPAC®, 2013. [Online]. Available from: A-Brief-Guide-for-Analysing-Electrodermal-Activity (biopac.com)

[30] H. F. Posada-Quintero and K. H. Chon, “Innovations in electrodermal activity data collection and signal processing: A systematic review,” Sensors (Switzerland), vol. 20, no. 2, 2020, doi: 10.3390/s20020479.

[31] Ledalab©, *Documentation*, Ledalab©. [Online]. Available from: www.ledalab.de/documentation.htm

[32] S. Lippé, M.-S. Roy, C. Perchet and M. Lassonde, “Electrophysiological markers of visuocortical development”, Cerebral Cortex, vol. 17(1), pp. 100-107, Jan 2007, doi: 10.1093/cercor/bhj130

[33] D. Fowles, G. Kochanska and K. Murray, “Electrodermal activity and temperament in preschool children”, Psychophysiology, vol. 37(6), pp. 777-787, Dec 2000, doi: 10.1017/S0048577200981836

[34] M. Shibagaki, T. Yamanaka and T. Furuya, “Effects of attention state on electrodermal activity during auditory stimulation of children”, Perceptual and motor skills, vol. 75(1), pp. 35-43, Aug 1992, doi: 10.2466/pms.1992.75.1.35

[35] K. G. Hernes, L. Mørkrid, A. Fremming, S. Ødegården, Ø. G. Martinsen and H. Storm, “Skin conductance changes during the first year of life in full-term infants”, Pediatric Research, vol. 52(6), pp. 837-843, Dec 2002, doi: 10.1203/00006450-200212000-00005

The Design and Testing of a Personalized Health Engagement Platform

A Case Study in Relationship-centered Innovation

Sara Chokshi
Healthcare Innovation and Technology Lab (HITLAB)
New York, USA
email: sak141@columbia.edu

Antoinette Schoenthaler
Dept. of Population Health, NYU Langone Health
New York, USA
email: Antoinette.Schoenthaler@nyulangone.org

Jeannette McClennan
The McClennan Group
New York, USA
email: jeannette@mcclennangroup.com

***Abstract*—Engagement remains a primary challenge to the adoption and success of public health interventions. Digital tools offer unprecedented capability to reach individuals where they live, even in underserved communities; however, lack of engagement is a persistent barrier to their effectiveness. Prior efforts at intervention and solution design attempt to employ a human-centered approach to address this challenge but have lacked the ability to use large data sets to both inform content and drive precision delivery of that content. Additionally, evaluation of the impact of these solutions takes a long time, hampering ability to test and tweak content and delivery strategies to achieve better engagement along the way. GoodLife Media's solution is a data-driven health participant engagement platform with dashboards for real-time monitoring of performance. This paper provides an overview of the GoodLife solution, the relationship-focused approach taken to its design, and the outcomes and learnings from the study of initial implementation.**

Keywords-health engagement; health communication; machine learning; human-centered design; innovation.

I. INTRODUCTION

Engagement remains a primary challenge to the adoption and success of public health interventions [1]. Research cites lack of personalization as a barrier to user engagement with digital health tools [2]. Prior efforts at intervention and solution design attempt to employ a human-centered approach to address this challenge but have lacked the ability to use large data sets to both inform content and drive precision delivery of that content [3][4]. Additionally, evaluation of the impact of these solutions takes a long time, hampering ability to test and tweak content and delivery strategies to achieve better engagement along the way.

Human-Centered Design as a best practice has at its core a focus on the patient's needs, motivations, and lifestyle [3][4]. The challenge remains exactly how to deliver solutions that yield the high rates of participant engagement necessary to deliver an intervention's intended results. Designed to address this challenge, the GoodLife Media^{TM} (GLM) platform is a precision communication solution powered by a novel card sorting game designed to collect end users' behavior, motivation and lifestyle data. It was developed by The McClennan Group [5], an innovation agency that creates digital health products and marketing programs for corporate clients such as IBM, AARP, Humana, Gilead, Vanguard, Blue Cross Blue Shield Carefirst, Partners in Primary Care, among others.

This paper outlines each component of the GoodLife solution, featuring the relationship-focused approach that drove the design of the platform and content strategy (Section II). Following is a brief description of the initial implementation of the platform presented as a case study (Section III) along with the evaluation of the platform's impact on average closure of care gaps for older adults receiving Medicare benefits (Medicare is a federally-funded program in the U.S. that provides health insurance coverage to individuals who are age 65 and over, and some people under age 65 with certain disabilities, including people with severe, end-stage kidney disease. Medicare Advantage refers to Medicare-approved health insurance plans from a private company providing health and drug coverage to the Medicare population) from a top five U.S. payor. We conclude (Section IV) by discussing future plans to adapt the platform to serve individuals from historically underserved communities.

II. GOODLIFE MEDIA SOLUTION

The GoodLife Solution aims to engage users while prompting and enabling them to take specific health-related actions. The solution consists of four major components: (1) engaging, data-driven personalized content fueled by a (2) behavioral science-informed strategy that leverages the engaging power of relationships, (3) bi-directional, omni-channel communication infrastructure, and (4) a comprehensive dashboard allowing for understanding of program progress on a variety of levels, identification of specific areas for intervention or shift in strategy, and design and testing of targeted campaigns aimed at specific participant segments or tasks.

 ISBN: 978-1-68558-004-9

A. Data-driven personalized content

The key to solving the personalization challenge lies in collecting hard-to-get datasets, including data on individual-level motivation & lifestyle. To accomplish this, we created a first of its kind card sorting game designed to collect hard to get non-clinical data in a fun and engaging way. It enjoys 86.5% completion rates, and it is the initial primary driver of the solution's personalized experiences. This device-agnostic card sorting game collects patients' behavior, lifestyle, and motivation with that challenge in mind, delivering as a result a Purpose Statement sentence consisting of their Talents, Passions, Impacts, Values, and Goals along with a compelling collage reflecting the output of the activity. As the target audience for the initial application of the solution was Medicare Advantage participants, the card sort activity was initially conceived in collaboration with colleagues at AARP's Life Reimagined Institute [6].

In our hypothesis, the benefit of using a card sorting activity in a health context points to theories of intrinsic motivation, which is central to one's engagement in and maintenance of health. Research has shown that tapping into patients' intrinsic motivation (acting for the inherent enjoyment of the activity involved) is the most autonomous form of motivation [7]. When the desired behavior is not inherently enjoyable (e.g. embarking on a restrictive diet), one may still be autonomously motivated through integrated regulation (i.e., acting in line with one's own goals and values).

B. Evidence-based behavioral science inspired content strategy

At its core, the GoodLife solution strategy is built upon evidence- both clinical evidence regarding healthful behavior as well as behavioral and social science principles proven to engage and impact the way that people conceptualize and address health-related issues. GoodLife's extensive Health Content Library contains a series of sequential communications designed to educate recipients around basic health-related topics (e.g. importance of blood pressure awareness) and principles of health management (e.g. annual wellness exams). Communications pathways are designed to be experienced as asynchronous, ongoing dialogues as one might enjoy with a trusted friend or care provider. The personalization as well as relationship focus of content are key to the GoodLife solution's content strategy.

To increase the impact of these dialogues, Health Content Library material is infused with behavioral economics inspired "nudges" based on the BASIC toolkit strategy for developing behaviorally informed interventions. Developed by the Organization for Economic Co-operation and Development (OECD), an international organization that works to build better policies for better lives, BASIC consists of four principles (Attention, Belief Formation, Choice, Determination) derived from the behavioral and social sciences—including psychology, cognitive sciences, and group behavior—to provide adopters with a step-by-step process for analyzing a problem and building strategic solutions [8]. Combining the power of analytics to personalize content and target the most prominent and costliest care gaps using behavioral economics enables us to increase our impact on member behavior in the areas that matter most to their health and well-being. Our systematic approach to developing and implementing these strategies allows us to monitor, test, and tweak tactics based on their success.

C. Bi-directional, omni-channel communication infrastructure

We used dynamic segments, generated by applying machine learning techniques to participant data, to drive communication plans in various ways (see Section III for details on techniques used). Firstly, dynamic clusters correlate directly to tone determined most likely to resonate with that segment. And each cluster is further segmented by conditions and healthcare gaps which drive overall content, subject lines, and call-to-action statements. Additionally, tones are constantly enhanced by how users respond to the communications. For example, if during our communications with a particular member we perceive a Social Determinants

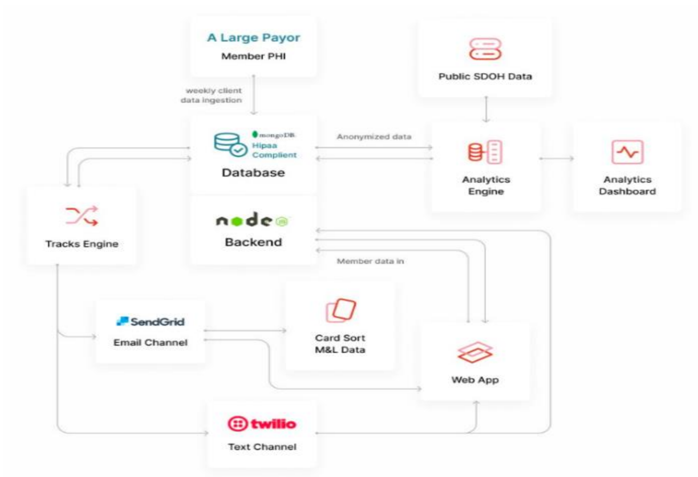

Figure 1. GoodLife Solution Infrastructure

Of Health (SDOH) barrier, messages will shift to conform to their reality. As a result, we produced 108 communication streams with bilateral capabilities, i.e., the ability to collect information from users along the way.

GoodLife's communication infrastructure is illustrated here (see Figure 1) and includes:

- SDOH data curated from public databases.
- An analytics engine designed to power our real-time Analytics Dashboard
- Member Personal Health Information (PHI), provided by the large payor every week and including claims data allowing us to measure gap closures.
- A Health Insurance Portability and Accountability Act of 1996 (HIPAA)-compliant database designed to

hold member PHI as well as the communication streams and card sorting data [9].

- SendGrid and Twilio implementations designed to maximize the deliverability of content by allowing for participants to seamlessly receive communications via text and/or email.
- A web application that provides users with a responsive experience, no app download needed.

As the participant experiences progress, we keep our stream of communication conversational by allowing them to provide us with self-reported data, including their personal goals, barriers, distractions, reasons for missed appointments, etc. Communication streams are built with trust and reciprocity at their core so that over time participants come to view communications from GoodLife as relevant and valuable- making clear there is "payoff" for every data point shared in line with that participants goals and values. We utilize simple, accessible language, avoiding jargon to ensure content is approachable and understandable at first read. Our range of strategically motivated formats is continuously evolving and includes:

- HIPAA-compliant bidirectional/conversational SMS (supports conversational tone).
- Talking Clinician Videos (authority or subject matter experts build credibility and trust).
- Storytelling/Animated Videos (supports understanding ideas in new ways)
- Cartoons/Webtoons (promotes relatability and playfulness)
- Emojis, Memojis (animation with authentic voices to make content easily digestible
- Stickers (supports peer to peer dissemination of simple calls to action)

We are constantly adding new formats as they are invented and tested. They are carefully selected based on project goals, the cohort's literacy level, age, call-to-action, and culture/language.

Figure 2: Real time dashboards illustrating participant program enrollment, status, and measure compliance

D. Real-time dashboards

Precision-communication demands increased rigor in measurements of results. The custom-built, real-time analytics dashboard delivers intelligence around key performance indicators and allows our partners to adapt and change direction as needed. The analytics dashboard can be accessed by a variety of users with various permissions levels and was designed to be standalone or integrated with our partner's system.

This first dashboard (right) image illustrates an overview of the population of the data, focusing on compliance for several healthcare measures. All the visuals are controlled by interactive filters that enable focus on specific groups within the population. This second dashboard image (left) features statistics around the different communications and activities, indicating how successful each campaign was in closing gaps. Other dashboards show detailed information regarding email delivery (e.g. sent, received, read) trended by date.

III. CASE STUDY: GOODLIFE APPLIED TO OLDER ADULT HEALTH ENGAGEMENT

In its first implementation, GLM partnered with a top five U.S. payor to apply the GoodLife solution to a group of older adult Medicare participants who were provided the opportunity to opt into communications from GoodLife as part of their regular benefits and communications from their payor.

Utilizing the latest data science techniques, including silhouette analysis and K-means [10], we created dynamic participant segments infused with insights generated from 101.9MM data points from 80 thousand members. These techniques were chosen for their ability to best utilize the card sort data to generate clusters that informed how participants would be segmented for targeted communications. K-means is a centroid-based clustering algorithm that identifies groups of program participants with common characteristics; Silhouette Analysis measures the distances between clusters, allowing us to divide participants into segments with the least amount of feature overlap between individuals in different clusters.

Using these techniques to combine card sorting output with payor provided SDOH and clinical data, we were able to generate insights on members' psychological drivers, preferences, attitude formation, and decision-making approach. Using this data-driven approach to communication and messaging, the GoodLife Solution delivered a personalized participant journey to 1000+ participants that directly addresses key challenges for public health programs: 1) relevance in messaging; 2) ability to address a broad range of psychosocial (i.e., depression), structural (i.e., transport), clinic-based (i.e., no access, waiting times, etc.), and other barriers (i.e., stigma and others, alone or in combination).

 ISBN: 978-1-68558-004-9

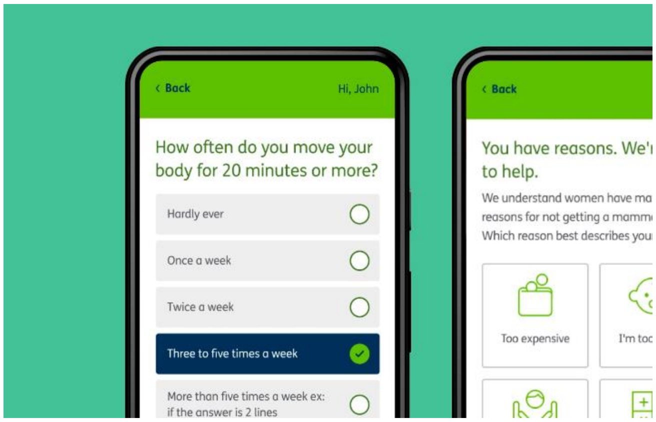

Figure 3: Example Communication

Evaluating Impact

To evaluate the impact of the program, two groups were set up: "test" group (exposed to standard Payor communications & GLM personalized content) and a lookalike "control" group (exposed only to Payor communications). Comparing these two groups provides insight into how effective the program is. To increase confidence in the ability to compare the two groups, additional analysis was performed to confirm the level of similarity between them.

To verify the effectiveness of our program, we designed a test to measure the higher gap closure rates among program participants. The gap closure rates for the test and control groups were compared for each measure, calculating the delta between each. The delta was then applied to the total group size for each measure to find the incremental gap closures, or the number of gaps closed in the test group due to the increased closure rates.

Our test results show both that there was an increase in gap closures among program participants and the increase in gap closures was statistically significant (at $p<0.05$) for 6 out of the 9 gaps. An average reduction in gaps of care of 9.4% was observed. In the case of breast cancer screening the reduction was more than 25% (26.89%). Chi-square analysis indicated that test and control groups were highly alike regarding their healthcare needs, further confirming findings of program effectiveness.

IV. CONCLUSION

This initial case study illustrates how, through s relationship-focused approach to design, along with data- and evidence-based development, the GoodLife Solution provides the foundation for a comprehensive program to reach, engage, educate, and sustain engagement of participants in their health behavior. In the future, applications of the GoodLife Solution will be applied as an engagement solution for members of historically underserved communities. The relationship-focus of the GoodLife solution, along with its modular infrastructure and tailorable content provides a strong foundation from which to build community and individual level engagement strategies.

REFERENCES

[1] S. O'Connor, P. Hanlon, and C. O'Donnel, "Understanding Factors affecting patient and public engagement and recruitment to digital health inventions: a systematic review of qualitative studies," BMC Med Inform Decis Mak, vol. 16, 2016, doi: 10.1186/s12911-016-0359-3

[2] C. Lyles, R. Watchter, and U. Sarkar, "Focusing on Digital Health Equality," JAMA, vol. 326, pp. 1795-1796, 2021, doi:10.1001/jama.2021.18459

[3] P. Koen, "Lean Startup in Large Enterprises Using Human-Centered Design Thinking: A New Approach for Developing Transformational and Disruptive Innovations," Howe School Research Paper, Jan 2015, doi:10.2139/ssrn.2556187

[4] T. Schulte and S. Bohnet-Joschko, "How can Big Data Analytics Support People-Centered and Integrated Health Services: A Scoping Review," Int J Integr Care, vol 16, June 2022, doi: 10.5334/ijic.5543.

[5] McClennan Group, [online] www.mcclennangroup.com [accessed October, 2022]

[6] AARP Life Reimagined Institute, [online] www.aarp.org/about-aarp/life-reimagined/ [accessed October, 2022]

[7] E. Deci, and R. Ryan, "Self-determination theory," in Handbook of theories of social psychology, P. Van Lange, A. Kruglanski, and & E. Higgins, Eds. New York: Sage Publications Ltd., pp. 416-436, 2012, doi:10.4135/9781446249215.n21

[8] OECD, "Tools and Ethics for Applied Behavioral Insights: The BASIC Toolkit," Paris: OECD Publishing, 2019, doi: 10.1787/9ea76a8f-en.

[9] HIPAA, [online] www.hhs.gov/hipaa/index.html [accessed October, 2022]

[10] D. Sharma, K. Thulasiraman, D. Wu, and J. Jiang, "Power Network Equivalents: A Network Science Based K-Means Clustering Method Integrated with Silhouette Analysis," Studies in Computational Intelligence, vol 689, C Cherifi, H. Cherifi, M. Karsai, and M. Musolesi, Eds. New York: Springer International Publishing, pp. 78-89, 2017, doi: 10.1007/978-3-319-72150-7_7

 ISBN: 978-1-68558-004-9